

Groundwater Research Report
WRC GRR 96-03

IMPACT OF TUNNEL DEWATERING ON SURFACE WATER BODIES IN
MILWAUKEE COUNTY: DETERMINATION OF HYDROGEOLOGIC
CONTROLS AND THE EFFICIENCY OF MONITORING ARRAYS

Douglas S. Cherkauer

1996

IMPACT OF TUNNEL DEWATERING ON SURFACE WATER BODIES IN
MILWAUKEE COUNTY: DETERMINATION OF HYDROGEOLOGIC
CONTROLS AND THE EFFICIENCY OF MONITORING ARRAYS

D. S. Cherkauer
Department of Geosciences
University of Wisconsin-Milwaukee

Groundwater Research Report
WRC GRR 96-03
University of Wisconsin System
Groundwater Research Program

Water Resources Center
University of Wisconsin-Madison
1975 Willow Drive
Madison, Wisconsin

1996

This project was supported, in part, by General Purpose Revenue funds of the State of Wisconsin to the University of Wisconsin System for the performance of research on groundwater quality and quantity. Selection of projects was conducted on a competitive basis through a joint solicitation from the University and the Wisconsin Departments of Natural Resources; Agriculture, Trade and Consumer Protection; Industry, Labor and Human Relations; and advice of the Wisconsin Groundwater Research Advisory Council and the with the concurrence of the Wisconsin Groundwater Coordinating Council.

ABSTRACT

The interaction of Milwaukee County's Northshore Tunnel with surface water bodies was analyzed. Seepage meter measurements established that the tunnel induced recharge into the dolomite and glacial aquifer of at least 1,600 m³/day from Lake Michigan and 534 m³/day from the Milwaukee River. Both fluxes contributed to a total flux to the tunnel on the order of 4,300 m³/day. The tunnel's influence extends up to 4 km away from it under the lake and about 2 km upstream in the river.

In surface water bodies near the tunnel, flow of water through the bed is a combination of vertical downward flow toward the bedrock system and the tunnel and lateral inflow from the unconsolidated sediments. The low conductivity Milwaukee Formation, topmost rock unit in most of the study area, restricts exchange between the sediments and rock, thus limiting the extent and magnitude of exchanges between tunnel and surface waters. It limits vertical outflow toward the tunnel and simultaneously causes groundwater in the sediments to flow predominantly horizontally to discharge in the lake or river. Locally this discharge can exceed any efflux induced toward the tunnel. High conductivity units, such as the Thiensville Formation, expand the extent of the tunnel's trough of depression. If such units are continuous between a surface water body and the tunnel's trough, they then increase the quantity of flow toward the tunnel. Thus accurate determination of the tunnel's impact requires a full understanding of the hydrogeologic system in which it's located and a well designed monitoring program.

The value of piezometers and seepage meters for determining the effect of a major groundwater stress on surface waters was assessed. Neither could accurately define the full extent and magnitude of the tunnel's influence by themselves, but they can be successfully combined in a scheme whose design is based on the characteristics of the hydrogeologic system. Piezometers provide necessary information on the distribution of heads and Ks, but are too expensive to be spaced densely enough to define the distribution of the tunnel's influence. Less conventional seepage meters can be deployed across the lake or river bed as densely as needed. They provide a cheap, accurate, and relatively rapid direct measure of the net flux across the bed.

CONTENTS

Abstract	ii
Figures	iv
Tables	vi
Introduction	1
Description of the Study Area	5
Hydrogeology	5
Tunnel System	9
Groundwater Heads	9
Methods	13
Piezometers	13
Seepage Meters	13
Digital Model	16
Results	17
Seepage Meters	17
Reproducibility	17
Correction for Non-simultaneous Readings	18
Control Site Observations on Lake Michigan	18
Time Correction of Observed Seepage	23
Exchanges between the Northshore Tunnel and Lake Michigan	24
Longshore Distribution of Seepage	24
Offshore Distribution of Seepage	24
Total Flow from Lake to Tunnel	28
Evaluation of Monitoring Methods	28
Exchanges between the Northshore Tunnel and the Milwaukee River	29
Distribution of Riverbed Seepage through Time	29
Distribution of Seepage along the River Channel	38
Evaluation of Monitoring Procedures	50
Digital Modeling	50
Procedures	50
Calibrated Results	52
Conclusions	61
Extent and Magnitude of Impacts	61
Hydrogeologic Controls on the Tunnel's Impact	61
Overall Assessment of Monitoring Methods	62
Recommendations	65
References	67

FIGURES

<u>Number</u>	<u>Page</u>
1 Location map of study area.	2
2 Locations of the primary tunnels in Milwaukee County relative to surface water bodies	3
3 Generalized stratigraphic column, Milwaukee County, Wisconsin.	6
4 Distribution of cores and packer tests used for this study.	7
5 Distribution of hydraulic conductivity and joint density within the dolomite aquifer by stratigraphic unit.	8
6 Hydrograph of a piezometer nest located at Locust Street and the Milwaukee River	10
7 Location map for piezometer nests and seepage meter sites in the Milwaukee River	14
8 Schematic of the University of Wisconsin-Milwaukee design seepage meter for shallow water.	15
9 The variation of rainfall, groundwater levels, and seepage through the summer of 1992 at the southern control site on Lake Michigan.	21
10 Composite distribution of the time-corrected seepages through the Lake Michigan bed.	25
11 Hydrogeologic cross-section from the Milwaukee River to Lake Michigan.	27
12 Seepages, heads, and hydraulic gradients at site 13, Kletsch Park, during summer, 1994	31
13 Seepages, heads, and hydraulic gradients at site 7, Estabrook Park South, during summer 1994	32
14 Seepages, heads, and hydraulic gradients at site 2, Data Management site, during summer 1994	33
15 Hypothetical relation between hydraulic gradient and seepage at a site with simple flow	36

16	Relation of seepage to vertical hydraulic gradient at Kletsch site, summer 1993	37
17	Relation of seepage to vertical hydraulic gradient at Estabrook South site, summer 1993	39
18	Relation of seepage to vertical hydraulic gradient at Data Management Site, summer 1993	40
19	Comparison of observed seepages and underlying geology along the Milwaukee River.	43
20	Comparison of calculated downward seepages with observed values from the Milwaukee River	48
21	Location of the finite difference grid for the model	51
22	Comparison of observed and modeled heads in bedrock	55
23	Comparison of observed and modeled heads in unconsolidated sediments	56
24	Distribution of simulated heads along Row 30 in calibrated model	57
25	Distribution of simulated heads along Row 45 in calibrated model	58
26	Offshore distribution of seepage as simulated by flow model	59

TABLES

<u>Number</u>	<u>Page</u>
1 Results of field tests to determine the error associated with mean fluxes using different numbers of lake seepage meters	19
2 Results of field tests to determine the error associated with mean fluxes using different numbers of river seepage meters	20
3 Seepages measured along Lake Michigan	26
4 Information on individual piezometers installed for this study	30
5 Frequency of negative seepages at sites 2, 7, and 13 on the Milwaukee River	34
6 Comparison of measured and inferred hydraulic conductivities at river seepage sites	41
7 Seepages along the Milwaukee River	44
8 Calculation of effective vertical leakance between the river and tunnel	46
9 Darcian calculation of flow to the Northshore Tunnel from the Milwaukee River .	47
10 Comparison of methods to calculate discharge to the tunnel from the Milwaukee River	49
11 Hydraulic conductivities used for the Northshore Tunnel simulation	53
12 Calibration targets for the finite difference model	54
13 Relative advantages and disadvantages of monitoring methods	63

INTRODUCTION

Until just recently, combined sewers in older parts of Milwaukee and Shorewood dumped raw waste into Lake Michigan and its tributary streams every time it rained. Prompted by court order, the Milwaukee Metropolitan Sewerage District (MMSD) opted to solve the problem by collecting combined sewage at the outfalls and then redirecting it to expanded sewage treatment plants (STPs). The crux of the solution is over 20 km of large diameter tunnels bored through bedrock and graded to the Jones Island STP. Stormwater is stored in the tunnels during wet periods, conveyed by the tunnels to Jones Island and treated when the STP has excess capacity.

Because these tunnels are constructed in a bedrock aquifer and operated as drains, they have a substantial impact on the groundwater system. It was the hypothesis of this study that they should then also have an impact on interconnected surface water bodies and that the extent and controls of that impact could be discerned.

This study was then conceived to address these objectives:

1. Define the extent and magnitude of the impact of the MMSD tunnels on Lake Michigan and the rivers in Milwaukee County (Figure 1);
2. Evaluate the hydrogeologic factors which control that extent and magnitude; and
3. Develop a protocol to maximize the effectiveness of monitoring arrays in detecting that extent and magnitude.

After the project was initiated it was realized that it would be more effective to concentrate efforts on just the Northshore Tunnel (Figure 2) and its interactions with Lake Michigan and the Milwaukee River. Access near the other tunnels for installing piezometers was too limited and the Menomonee and Kinnickinnic Rivers are often concrete lined, thus the project was conducted to address the objectives in a narrower study area.

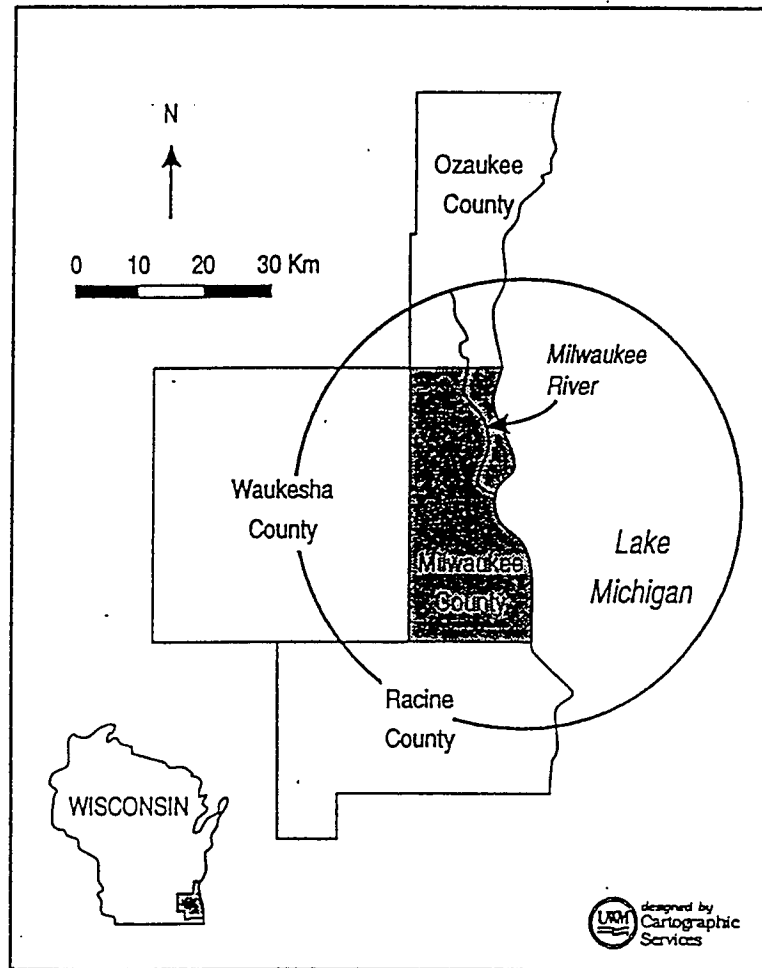


Figure 1. Location map of study area.

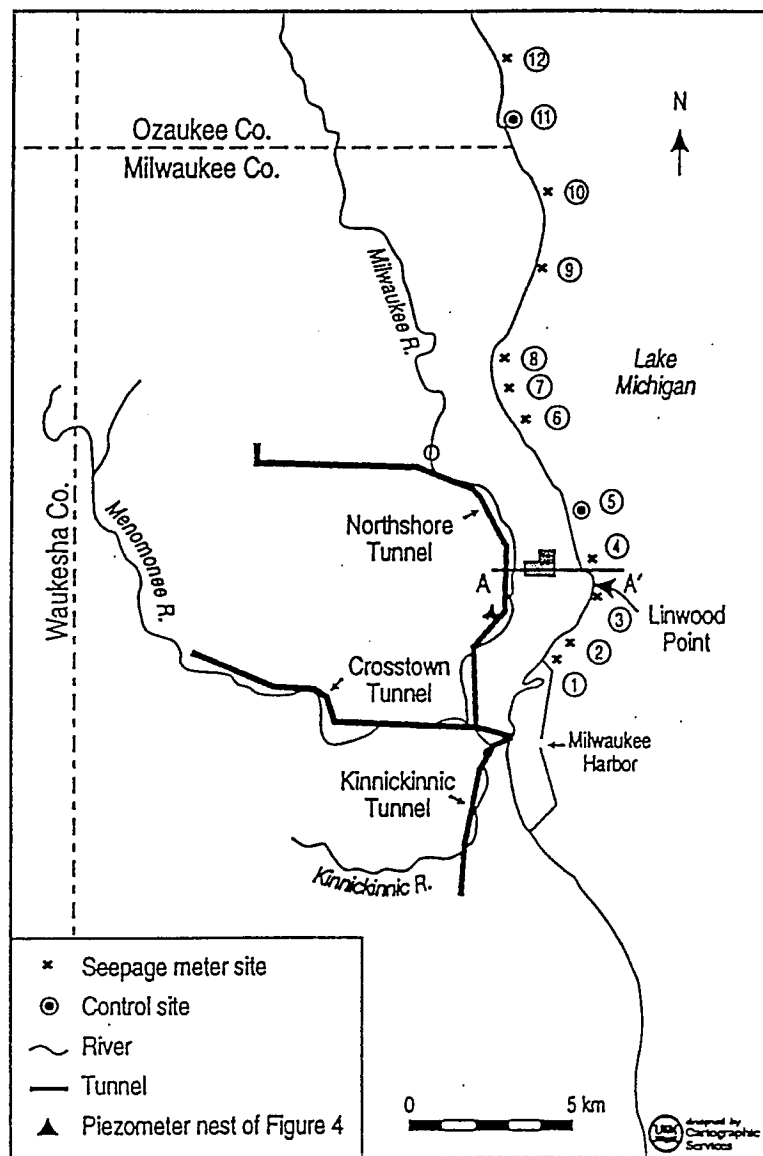


Figure 2. Locations of the primary tunnels in Milwaukee County relative to surface water bodies. Seepage meter positions occupied on Lake Michigan are shown. Line A-A' is position of Figure 11. Shaded area on Line A-A' is University of Wisconsin-Milwaukee campus.

DESCRIPTION OF THE STUDY AREA

HYDROGEOLOGY

The uppermost aquifer beneath the study area is a combination of Silurian and Devonian age dolostones and Quaternary age unconsolidated sediments. It is separated by the Maquoketa Shale (Ordovician) from a deeper aquifer consisting dominantly of Cambrian age sandstones. Because the tunnels and the surface water bodies of interest lie in the upper aquifer and because the Maquoketa functions as an aquitard, this study has concentrated exclusively on water exchanges between the upper aquifer and surface water bodies near the tunnel.

The Silurian and Devonian stratigraphy of the study area is presented in Figure 3. Bedrock units dip eastward toward the Michigan Basin at less than 3° . The units vary in thickness throughout and also pinch out toward the west due to glacial erosion. Thicknesses of geologic units beneath the land surface are well-defined because of an extensive coring program associated with tunnel construction. The distribution of rock units beneath the lake is conjectural, based entirely on extrapolation of the onshore geology offshore.

Rovey (1990) and Rovey and Cherkauer (1994a) have demonstrated that the hydraulic conductivity of the bedrock units varies in a predictable manner. As part of the pre-tunnel coring program, the MMSD conducted hundreds of pressure drill-stem tests (commonly called packer tests). Each test packs off a 7.6-m (25-foot) interval of rock and injects water into it at a known pressure. Observation of the flow during injection allows calculation of hydraulic conductivity for the interval. Figure 4 shows the distribution of coreholes and packer tests which form the database. When the test values are grouped by stratigraphic unit, they reveal a consistent pattern (Figure 5a).

Dolostones which were originally deposited in shallow seas are relatively coarse-grained deposits such as wackestone, packstones, and boundstones, have hydraulic conductivities on the order of 10^{-4} to 10^{-3} cm/sec (Figure 5a). In contrast, dolostones which were deposited in deep water produced carbonate mudstones or even shales, which have hydraulic conductivities of $\sim 10^{-6}$ cm/sec (Figure 5a). In addition, there is a 5- to 10-m thick weathered zone atop the bedrock. Because dolostone is water soluble, extensive weathering increases its porosity and thus, hydraulic conductivity.

It remains controversial whether the pattern observed in Figure 5a is the result of primary or solution-enlarged porosity within the units or mechanical discontinuities (breaks) in the rock. Figure 5b provides one measure of the frequency of breaks in the rock units (joints observed in the cores). This measure shows little correlation to the observed distribution of hydraulic conductivity. Other studies suggest that the dolostone's hydraulic properties are probably a combination of porosity and fracture effects.

The distribution of conductivities shown in Figure 5a has been used as the operating model for the hydraulics of the dolostones in this study. More details on the development and analysis of the data are available in Rovey and Cherkauer (1994a, b) and Rovey (1990). Measured

Devonian	Milwaukee	Lindworm
		Berthelet
	Thiensville	
Silurian	Waubakee	
	Racine	Undifferentiated
		Romeo
	Manistique	Waukesha
		Brandon Bridge
		Franklin Quarry
	Byron	
	Mayville	

Figure 3. Generalized stratigraphic column, Milwaukee County, Wisconsin. The primary subdivision is at the formation level. Subdivisions at the member level are informal, except within the Milwaukee Formation. Based on Rovey (1990), modified from Mikulic (1977) and Ostrom (1967).

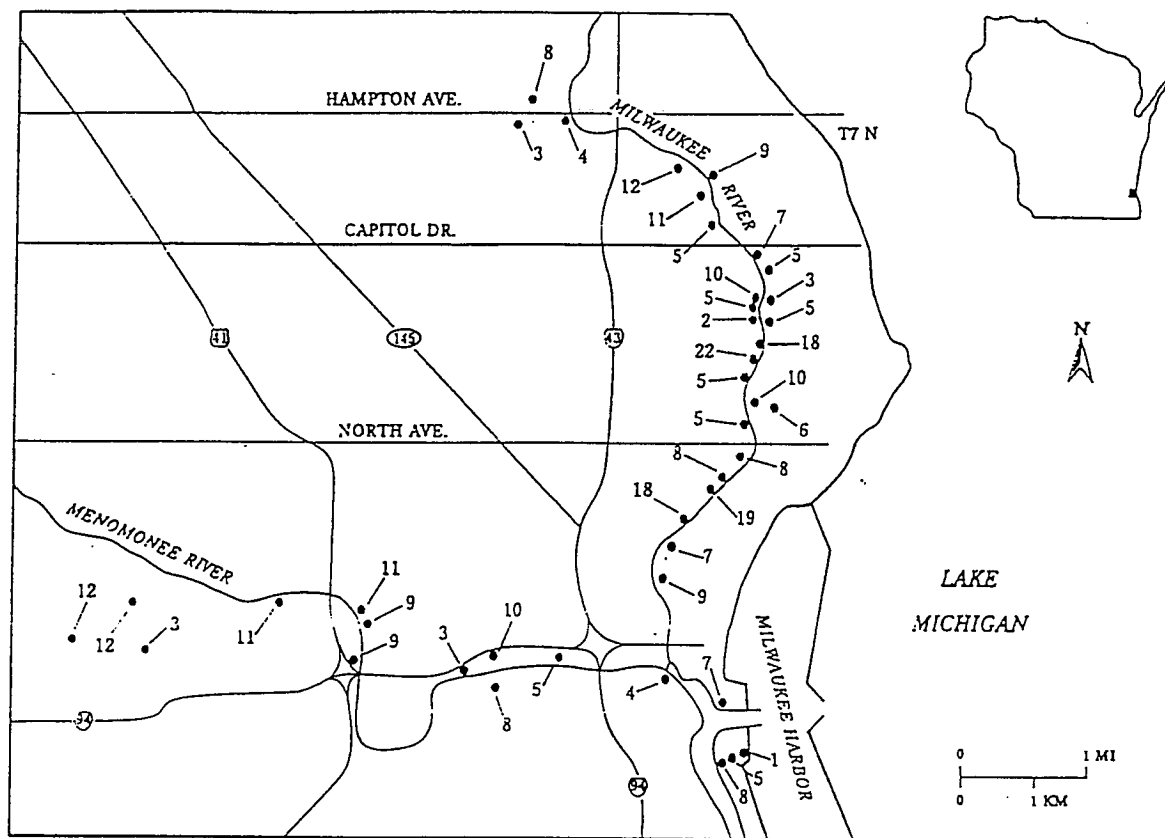


Figure 4. Distribution of cores and packer tests used for this study. Each dot represents a core drilled by the Milwaukee Metropolitan Sewerage District. The value adjacent to it is the number of packer tests conducted in that hole which straddle a single stratigraphic unit.

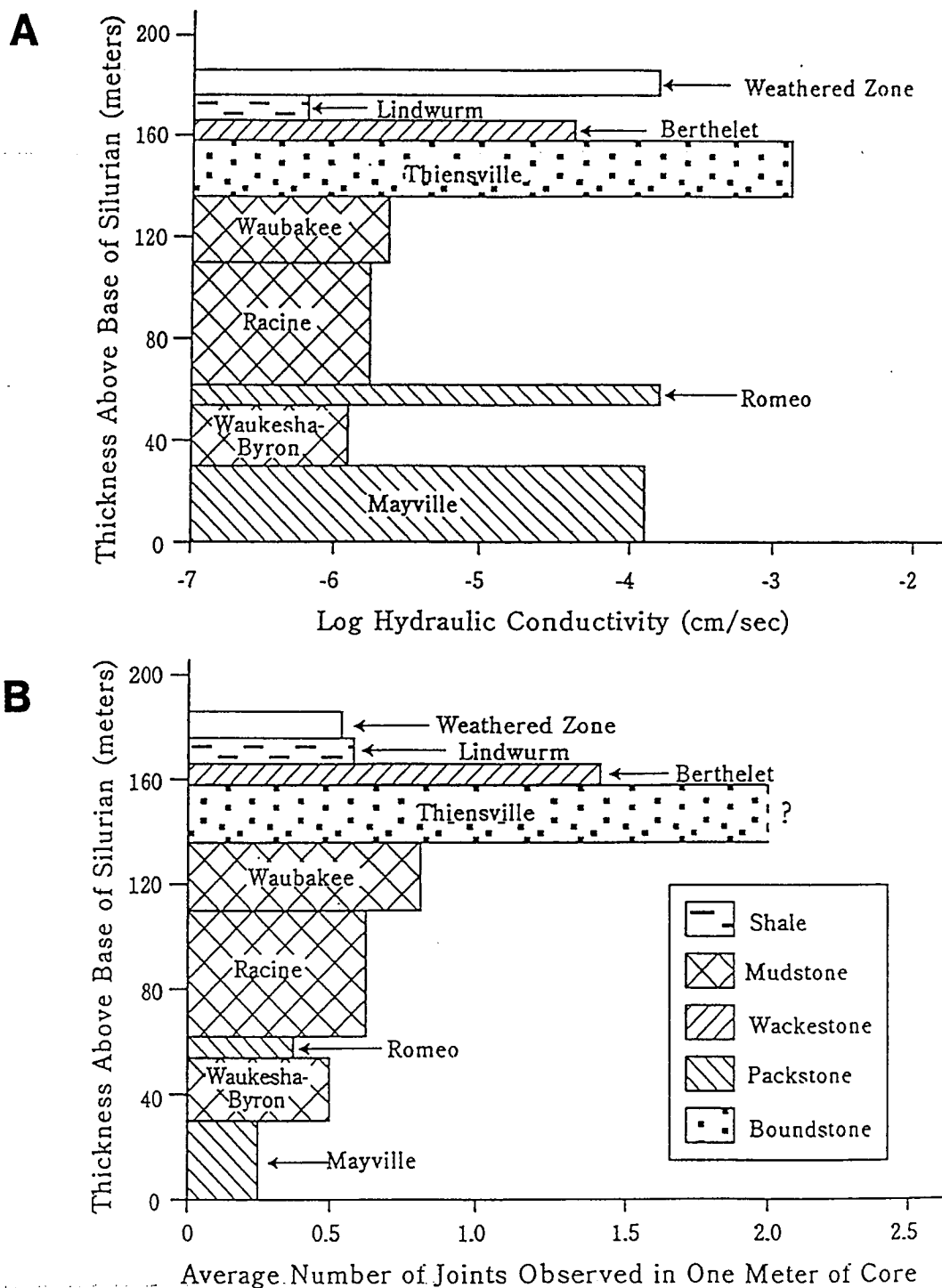


Figure 5. Distribution of hydraulic conductivity and joint density within the dolomite aquifer by stratigraphic unit. Each bar is the average thickness of a particular unit and extends to the geometric and arithmetic means, respectively, of each unit's hydraulic conductivity and joint density. The patterns depict the dominant texture of each unit. A - Hydraulic conductivity (Milwaukee Metropolitan Sewerage District, 1981, 1984a, b); B - Original results were presented as joints per successive 5-foot increments. Most Thiensville values, however, were recorded as >6 joints/5 feet. (Note that the Lindworm and Berthelet shown here are members of the Milwaukee Formation, while the Romeo Beds are the lowest member of the Racine Formation.

conductivities are scale dependent (Rovey and Cherkauer, 1995), so those in Figure 5 are valid only for the 8-m scale at which they were obtained.

The unconsolidated sediments range from glacial tills and outwash of Pleistocene age to modern lacustrine, estuarine, and fluvial sediments. No attempt was made to map or correlate these materials; instead, site-specific or published (Rodenback, 1988) hydraulic conductivities were used where appropriate.

TUNNEL SYSTEM

A set of storage-conveyance tunnels has been constructed by MMSD within the dolostones of the uppermost aquifer (Figure 2). This study concentrates on the Northshore Tunnel because of its proximity to Lake Michigan and the Milwaukee River and because public land along its route allowed access for the installation of piezometers and seepage meters.

The Northshore Tunnel is 5.2 m (17 feet) in diameter to the north and west of the arrow pointing to it in Figure 2 and 9.1 m (30 feet) in diameter to the south. It is designed to function as a gravity drain graded to flow south to a connection with the Crosstown and then east to a sewage treatment facility on Milwaukee Harbor. It was bored primarily in the Waubakee and Racine Formations (Figure 5) because of the formation's structural integrity and low conductivity.

Because of its gravity drainage design it is constructed beneath the Milwaukee River along much of its length, as this is where the combined sewer system delivers its load. The tunnel is inlined, but extensive grouting was done along its interior after it was bored. Accumulated water in the tunnel is pumped out for treatment to maintain an inward hydraulic gradient.

GROUNDWATER HEADS

The impact of the tunnel on heads in the shallow groundwater system has been pronounced (Figure 6). The response at the nest shown in Figure 6 is typical. Prior to tunneling, heads in the groundwater system were above the level of Lake Michigan, but with a slight downward vertical component, indicative of flow toward the lake. When tunneling began in 1987, the tunnel served as a new discharge stress on the aquifer and heads began to drop. As construction continued and a greater tunnel length was opened, heads continued to decline right up until construction was completed in 1991. Note that the tunnel is located in the Racine Formation 85 m (279 feet) below the surface of Lake Michigan at the nest in Figure 6 and it generates a consistent downward gradient (heads decrease downsection from glacial to Milwaukee to Thiensville to Racine).

After boring was complete, leaking portions of the Racine Formation were grouted from the tunnel's interior. This action caused the rebound in heads observed after 1991 (Figure 6) and accounted for the reduction of the head difference between the Milwaukee and Racine Formations at this site.

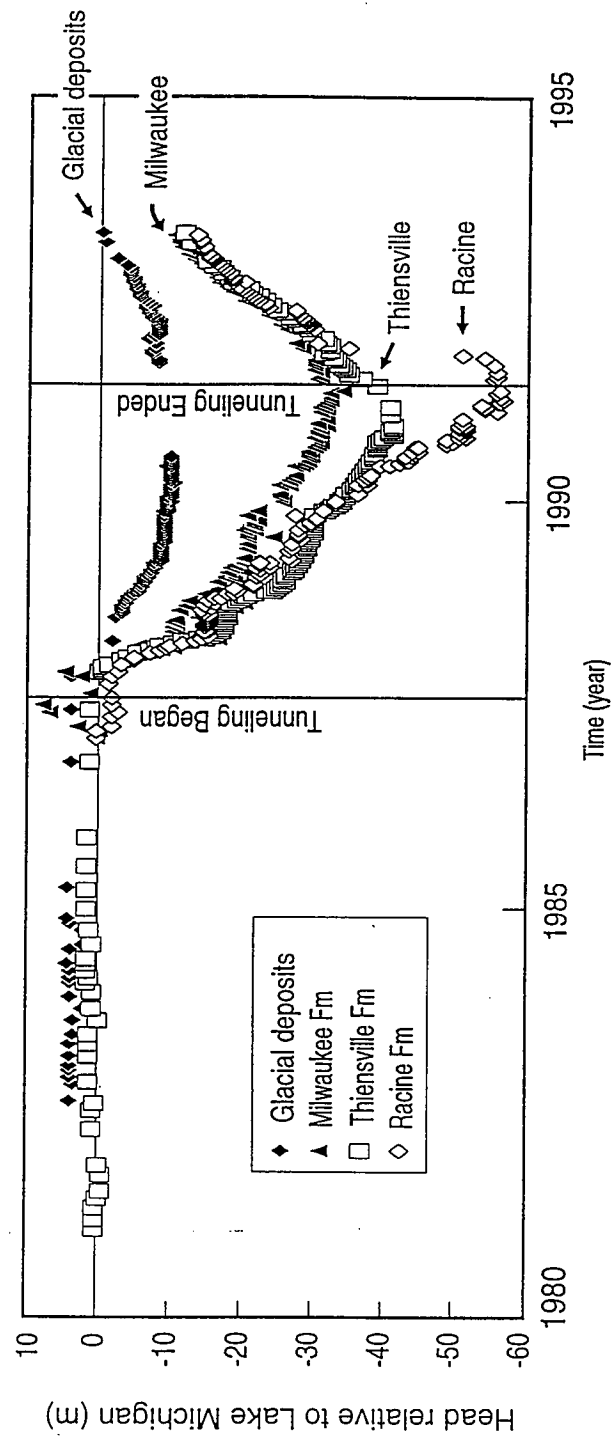


Figure 6. Hydrograph of a piezometer nest located at Locust Street and the Milwaukee River. Site location is shown on Figure 2. Relative positions of rock units are shown on Figure 3. Glacial sediments overlie the rock.

Heads stabilized at the 1993 levels until the tunnels were activated in 1994. Under stable conditions there was still a downward vertical gradient and heads throughout most of the unconsolidated deposits had risen above the level of Lake Michigan.

Because many structures in downtown Milwaukee are built on wooden pilings in fill atop estuarine deposits, MMSD needed to keep the unconsolidated sediments from dewatering there. As a consequence, they operated injection wells in the sediments along the southernmost 2 km of the Northshore Tunnel. The nest in Figure 6 was unaffected by the injection, which had the effect of presenting much drawdown in the sediments at the tunnel's southern extremity.

The MMSD measured the flow of water in the tunnel before it was connected to the sewer system and after grouting was completed. For the reach where the Northshore is under the Milwaukee River (from Hampton Avenue on the north to its convergence with the Crosstown on the south), 4,300 m³/day was entering the tunnel in late 1992. This inflow was all groundwater drainage at the time, with some coming from artificial recharge via injection wells, some from natural recharge, and the rest from induced recharge from Lake Michigan and the Milwaukee River.

METHODS

To determine the extent and magnitude of the tunnel's impact on surface waters three approaches were taken. Heads were measured in piezometer nests to define hydraulic gradients and flow directions. Fluxes across the beds of Lake Michigan and the Milwaukee River were measured directly with seepage meters. Finally, a digital flow model was constructed for the study area to allow more thorough interpolation between the site-specific field measurements.

PIEZOMETERS

The MMSD has constructed and monitors 10 piezometer nests along the length of the Northshore Tunnels (Figure 7). These piezometers are screened primarily in bedrock between the elevation of the crest of the tunnel and the base of the unconsolidated sediments. They provide excellent information on the distribution of heads in bedrock along the tunnel, but suffer from two shortcomings. First, there are very few located away from the tunnel (Figure 7), so they provide little information on the lateral extent of tunnel impact. Secondly, they are usually not constructed in a manner which will provide much information about flow in the unconsolidated sediments or between the sediments and the river. They are commonly screened across very long intervals, and there are never nested pairs of them in the sediments.

As part of this project, additional piezometer nests were installed in the sediments (Figure 7) with several goals in mind:

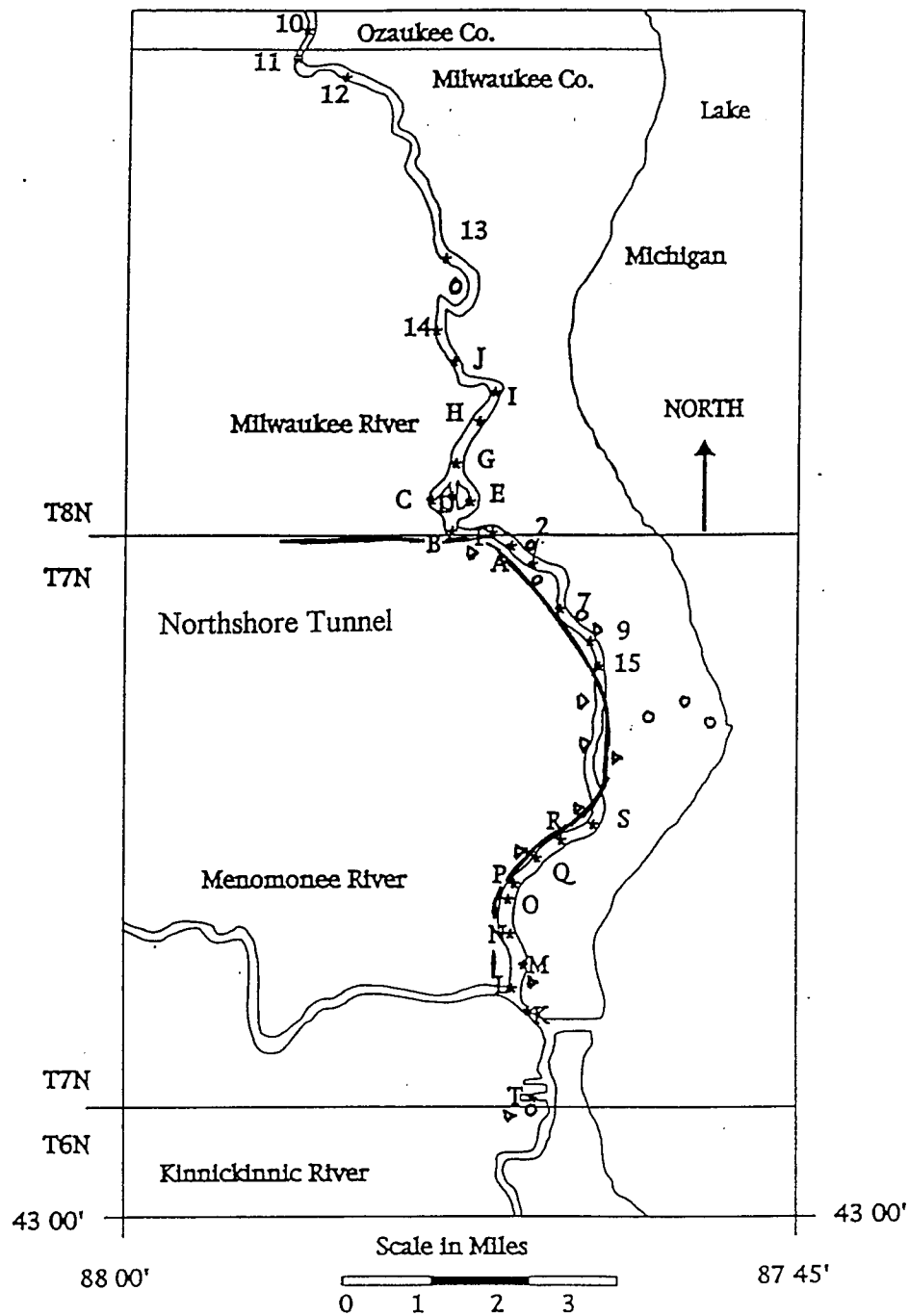
1. Determine head distributions in the sediments adjacent to the river and lake;
2. Provide control information along the river away from the tunnel; and
3. Provide head control transverse to the orientation of the tunnel.

Eighteen piezometers were installed in the sediments, primarily on state and county land.

SEEPAGE METERS

Seepage meters are devices designed to directly measure the flux of water across the sediment-water interface in a surface water body. Several variations of the University of Wisconsin-Milwaukee design (Figure 8) were used in this study. The shallow water meter is designed for use where an individual can carry them to a location in a stream and reach the streambed by hand. For deeper river sections, a modification of this design was used, which can be set and electrically activated from a boat (Camber, 1994). These two designs weigh 7 to 10 kg and are referred to as river meters in this report. For work on Lake Michigan, a much larger and heavier (70 to 90 kg) version (Cherkauer and McBride, 1988) was used. They are referred to as lake meters in this report.

Meters were installed at 28 sites along the Milwaukee River (Figure 7) to determine the spatial distribution of seepage. In addition, five sites (13, A, 2, 7, and 9) were monitored repeatedly over 2- to 3-month periods to examine temporal variation in seepage. Four of these sites (all except 9)



- * Seepage meter location (Camber, 1994) ○ Piezometer nest (this study)
 ▷ Milwaukee Metropolitan Sewerage District piezometer nest
 _____ Position of North Shore Tunnel 10 Shallow water meters
 J Deep water, electrically activated meters

Figure 7. Location map for piezometer nests and seepage meter sites in the Milwaukee River.

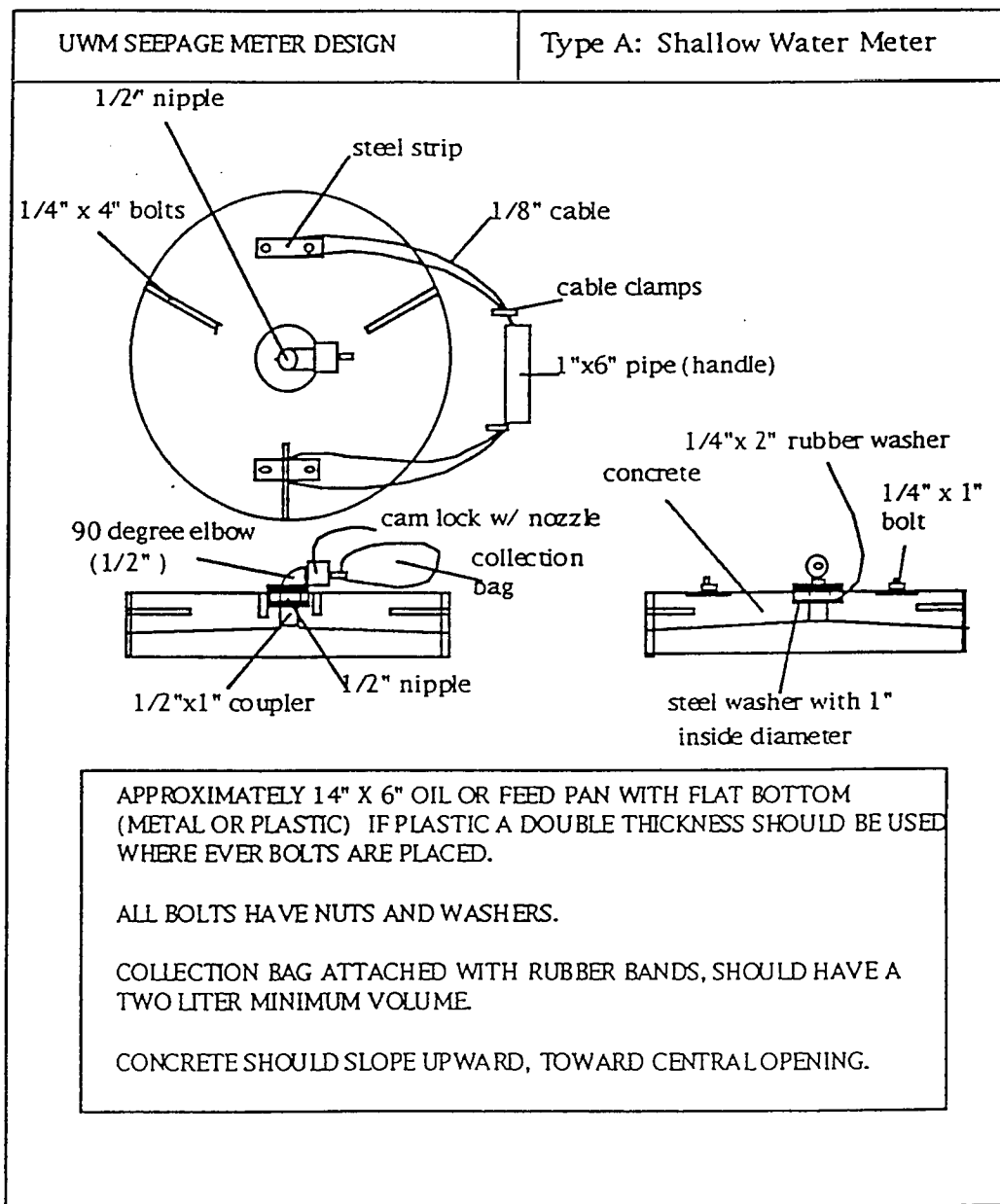


Figure 8. Schematic of the University of Wisconsin-Milwaukee design seepage meter for shallow water. Total weight is 7 to 10 kg. This meter is installed by a person wading in a stream.

are directly adjacent to onshore piezometer nests. Staff gages to record river levels were also installed at these sites.

Lake meters were set at 12 sites along 16 km of shore north from Milwaukee Harbor (Figure 2). At each site, they were deployed in transects of three to seven measurement positions aligned perpendicular to shore and spread over the first 1 to 2 km from shore. In most instances on Lake Michigan, the meters must be in place 7 to 10 days to make an accurate measurement.

DIGITAL MODEL

In order to merge field observations of heads and fluxes with hydrostratigraphical information and test the sensitivity of the tunnel impact to hydrogeologic conditions, a digital simulation of groundwater flow in the study area was developed. The code MODFLOW (McDonald and Harbaugh, 1984) was used because it is fully three-dimensional and because it handles groundwater/surface water interactions well.

Unconsolidated sediments were simulated as two active layers (glacial till and river deposits, both outwash and modern alluvium). Bedrock was simulated as six active layers (Milwaukee, Thiensville, Waubakee/Racine, Romeo, Manistique, and Mayville). The weathered zone has been incorporated in the high conductivity unconsolidated sediments (Layer 2). The Milwaukee River, Lake Michigan, the Northshore Tunnel, known injection wells, and surface recharge were simulated as stresses to the model. The contacts between geologic units, determined from the cores in Figure 4 and other drilling data, were input as layer tops and bottoms and held constant.

The study area was overlain by a grid of 87 x 64 nodes, with nodal size over the tunnel being 100 x 200 m. Lateral boundaries were conceptualized as no flow far out in Lake Michigan and parallel to known flow lines, and specified flux everywhere else. The fluxes were obtained from Darcian calculations using known gradients and the simulated layer transmissivities.

The model was calibrated to target fluxes and heads by varying surface recharge, the vertical and horizontal hydraulic conductivities of layers, the leakance of the lake and river beds, and the conductance of the tunnel. As much as possible, the varied properties were held spatially constant throughout the model. After calibration the model was used to check the extent of the tunnel's impacts observed with the piezometers and seepage meters and then to determine the sensitivity of those impacts to the varied properties.

RESULTS

SEEPAGE METERS

Reproducibility

Seepage meter readings contain uncertainties resulting from instrument bias and improper setting as well as from spatial and temporal variability of the flux being measured. Instrument bias is a determinate error which has been quantified in laboratory tests (McBride, 1987). The field readings must be corrected for the hydraulic inefficiency of the meters themselves and the effects of settling into sediment.

These corrections were performed as described in Cherkauer and McBride (1988). Belanger and Montgomery (1992) recently confirmed that the hydraulic inefficiency of seepage meters is significant. In this study, the meters are 62% efficient in the range of seepage rates measured. McBride (1987) conducted 60 tests of meter efficiency in the laboratory which established that the 95% confidence interval is $62 \pm 3\%$. Camber (1994) showed that the deep and shallow water river meters have the same hydraulic efficiency, despite somewhat different plumbing designs. This settling effect is minimal if the meters are allowed to equilibrate for at least 30 min. before activation (Cherkauer and McBride, 1988).

Hydraulically corrected seepages are calculated as:

$$q_c = \frac{V_1 / t}{(A) (ME)} \quad (1)$$

where:

- q_c = seepage rate corrected for meter inefficiency (ml/hr/m²),
- V_1 = volume of water gained or lost in the collection bag (ml),
- t = time over which measurement made (hours),
- A = cross-sectional area of the seepage meter (m²), and
- ME = meter efficiency (%).

The total determinate error on q_c is $\pm 5\%$ (95% confidence).

The uncertainty introduced to the seepage value by incomplete seating of the meter in the sediment or random fouling of the plumbing by organisms or sand was measured by placing five lake meters as close together on the lakebed as possible without their instrument cables intertwining. After 4 days on the lakebed, the five meters recorded a mean seepage rate of 5.20 ml/hour/m² with a standard deviation of 0.55. The recorded values were then grouped into all possible combinations of 2, 3, and 4 readings to provide a bootstrap estimate of the error (at 95% confidence) associated with using 2, 3, or 4 seepage meters at a site to establish a mean flux. The results of this test indicate

that a flux based on a single meter reading is good to $\pm 15\%$, but the error drops to $\leq 5\%$ if two or more meters are used (Table 1).

This high accuracy is believed to be the result of the lake meter design. As indicated previously, these meters weigh > 70 kg and have a reinforced rim of sharpened steel which is forced deep into lakebed sediments by the meter's weight. The meters only fail to function well in areas of cobbles or larger particles (where they cannot seat fully) or on soft sediment (where they continue to sink while deployed).

Camber (1994) has conducted similar tests on the smaller river seepage meters. Six meters were placed across the width of the channel at site 2 (Figure 7). They measured a mean seepage rate of 78.6 ml/hour/m^2 , with a standard deviation of 33.4. The high variability is the result of spatial differences of seepage across the channel and measurement uncertainties associated with the individual meters. The bootstrap calculations show that the mean seepage on a channel transect cannot be accurately determined by a single meter (49% error, Table 2). However, if two or more meters are used, the mean seepage can be determined with $< 13\%$ uncertainty (Table 2).

Correction for Non-simultaneous Readings

Because the limited number of seepage meters made it impossible to monitor all sites on the lake or river simultaneously, control sites were established at which continuous measurements were taken. For the lake and river, two meters were installed permanently for each summer of observation at control sites, while the remaining meters were deployed at other locations. After 7 to 10 days on the lake and 3 to 5 days on the river, all meters were retrieved for measurement. Then the control site meters were reset in position and the others were moved to another site.

Because seepage rates at a location vary through time in response to changes in groundwater levels, measurements taken at different times must be corrected to remove the effects of temporal variations before they can be compared. The control sites provided the data for this time correction. The uncertainty associated with this correction is not known, but is estimated to be on the order of 20%.

Control Site Observations on Lake Michigan. The northern control site (Figure 2) is more protected and was used when measurements were conducted along the entire length of the study area in order to establish the north-south extent of the tunnel's effect. When it was decided to concentrate measurements within the zone of the tunnel's influence in order to better define its shape, the control site was relocated southward so that it would be centrally positioned.

Seepage, after hydraulic correction via Equation 1, changed through time at the southern control site (Figure 9c). The two seepage meters were located 100 and 200 m from shore at depths of 2 and 3 m, respectively. In late May and early June, both meters consistently showed negative seepages, flow from the lake downward into the aquifer, as was expected. Nearshore seepage was more strongly downward than that offshore (Figure 9).

Table 1. Results of field tests to determine the error associated with mean fluxes using different numbers of lake seepage meters.

Number of Seepage Meters in a Sample†	Number of Combinations	Mean Seepage (ml/hr/m ²)	Standard Deviation*	t_{95} (t Statistic for 95% Confidence)**	95% Confidence Interval	
					(Absolute)	(As % of Mean)
1	5	5.20	0.55	2.78	0.76	15
2	10	5.20	0.34	2.26	0.26	5.0
3	10	5.20	0.23	2.26	0.17	3.3
4	5	5.20	0.14	2.78	0.19	3.7

- * The standard deviation listed is that for the distribution of the means of each of the groups of a given size about the mean of 5.20.
- ** The confidence interval has been calculated as $[(t_{95})(s)/(n^{1/2})]$, where n is degree of freedom. It is interpreted to mean that there is a 95% probability that the true seepage falls within the range of the mean \pm the confidence interval.
- † Only five seepage meters were used in the test. The results from those meters have then been artificially grouped in all possible combinations of 1, 2, 3, and 4 meters.

Table 2. Results of field tests to determine the error associated with mean fluxes using different numbers of river seepage meters.

Number of Seepage Meters in a Sample†	Number of Combinations	Mean Seepage (ml/hr/m ²)	Standard Deviation*	t ₉₅ (t Statistic for 95% Confidence)**	95% Confidence Interval	
					(Absolute)	(As % of Mean)
1	6	78.6	33.4	2.57	38.4	49
2	15	78.6	20.0	2.15	9.9	12.5
3	20	78.6	14.0	2.09	6.7	8.5
4	14	78.6	9.4	2.16	5.6	7.2

* The standard deviation listed is that for the distribution of the means of each of the groups of a given size about the mean of 78.6.

** The confidence interval has been calculated as $[(t_{95})(s)/(n^{1/2})]$, where n is degree of freedom. It is interpreted to mean that there is a 95% probability that the true seepage falls within the range of the mean \pm the confidence interval.

† Only six seepage meters were used in the test. The results from those meters have then been artificially grouped in all possible combinations of 1, 2, 3, and 4 meters.

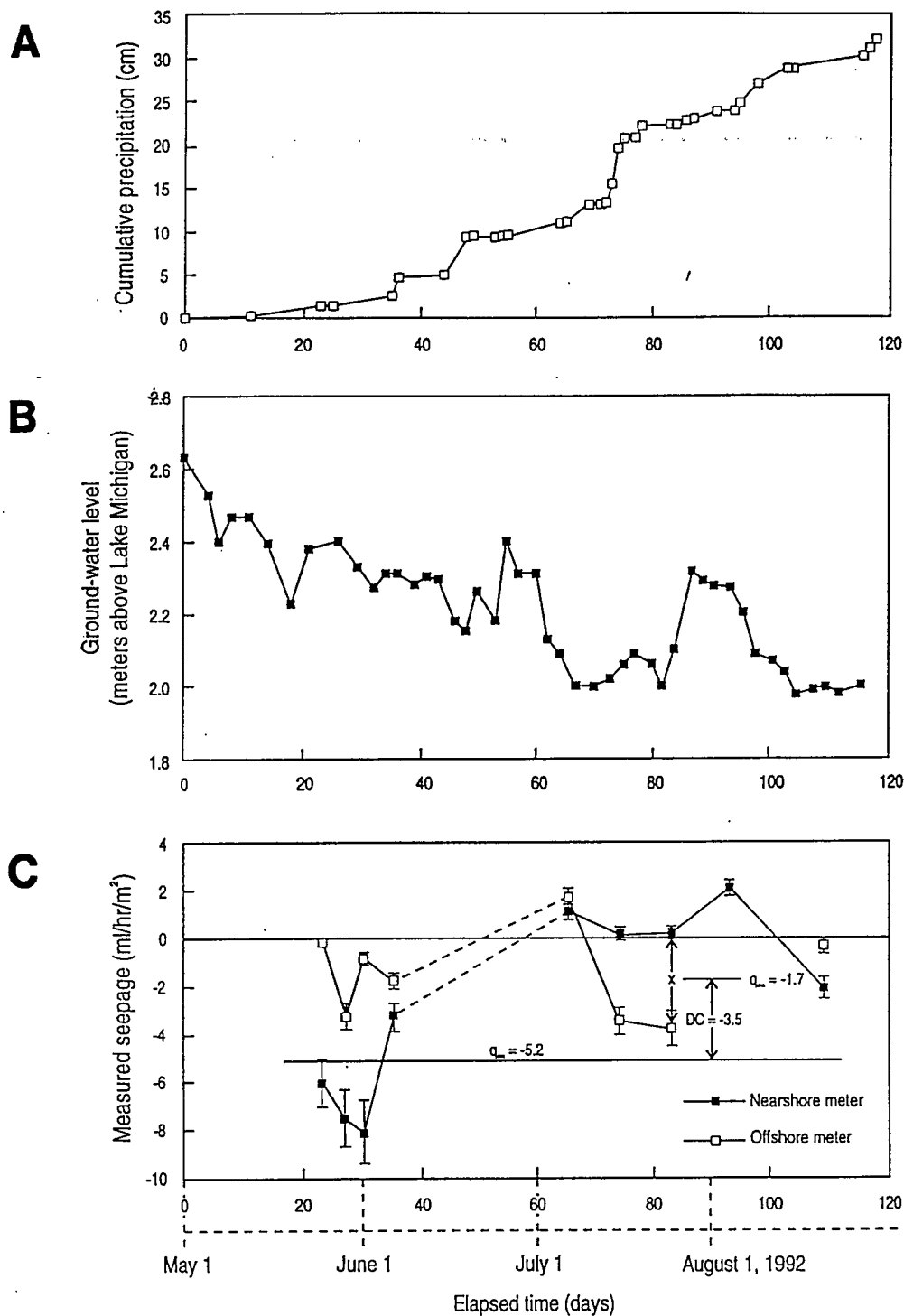


Figure 9. The variation of rainfall (A), groundwater levels (B), and seepage © through the summer of 1992 at the southern control site on Lake Michigan. Control location is Site 5 on Figure 2. Seepages are plotted in the middle of the period of measurement, with negative values signifying downward seepage toward the tunnel. The offshore meter failed during the second last period, so no data point is plotted. Time corrections make all average readings at the control site conform to the date with minimum rainfall effect ($q_{cm} = -5.2$ on day 27). An example correction using Eq. 3 is shown for day 83. Error bars are for 95% confidence interval for a single meter (Table 1).

Problems with the research vessel required a shutdown from June 8 to July 1, 1992 while arrangements for a replacement vessel were made. Subsequent to resumption of the measurements, an unanticipated change occurred. Positive seepages (upward into the lake) became prevalent nearshore, even though this site is within the zone of influence of the tunnel and water levels in the underlying Thiensville Formation are below lake level. Comparison of rainfall and groundwater levels to the seepages reveals the cause. Two major rainfall events occurred during the study period, on June 17 and July 13, 1992 (days 46 and 73, respectively, on Figure 9a). They were followed after a lag of about 10 to 15 days by increases at days 56 and 87, respectively (Figure 9b) in the water level of the control piezometer (screened in sandy glacial deposits at a location 100 m inland and 6 to 8 m below the lake surface). These increases in the water table elevation were then followed, after another lag of 10 to 12 days, by the peaks in positive seepages (days 66 and 93, respectively, on Figure 9c). Evidently, rainfall causes recharge to the unconsolidated sediments from which water flows laterally to the lake. The effect is relatively short-lived, especially at the position of the offshore seepage meter (Figure 9a).

These observations support a conceptual model of the flow in which there is a continuous (and relatively steady) seepage out of the lake toward the tunnel coupled with a more ephemeral in-seepage from the unconsolidated materials. The seepage meters at the control site are measuring a net combination of these two fluxes at any time, with:

$$q_{\text{net}} = q_{\text{in}} - q_{\text{out}} \quad (2)$$

where:

- q_{net} = Seepage observed in a seepage meter;
- q_{in} = Inward flow (positive seepage) to the lake from unconsolidated sediments; and
- q_{out} = Outward flow (negative seepage) to the Thiensville Formation and the tunnel.

At the southern control site, the observed seepages were predominantly downward (Figure 9c), induced toward the underlying Thiensville Formation and thus the tunnel by a downward hydraulic gradient. After extended dry periods (days 20 to 40 on Figure 9), the seepage toward the tunnel is greater nearshore than offshore because the former position is closer to the tunnel and has a stronger downward gradient.

After recharge events, however, the net seepage becomes less negative, sometimes even changing to positive (toward the lake) as the in-seepage from the unconsolidated materials dominates. The positive net seepages seem to occur more quickly and to persist longer at the nearshore position (Figure 9c), probably because it's closer to the source of the influx. Unfortunately, the control site data are of insufficient resolution to accurately track the decay of a recharge surge as it dissipates offshore.

Three points should be emphasized here. First, the seepage readings plotted in Figure 9c show that net flux through the lakebed at control site 5 is predominantly out of Lake Michigan. Second, this occurs despite the fact that the tunnel inducing that outseepage is > 2 km away and the lake is separated from the conductive aquifer by > 20 m of low conductivity sediment and 12 m of shale at

that point. Third, the control site observations indicate that significant temporal variations of the net seepage at a site occur in response to rainfall and that these must be removed before measurements taken on different dates can be compared directly.

Time Correction of Observed Seepage. The control data were used to correct all individual seepage measurements on the lake to what they would have been if they all had been taken for a synchronous period. This was done by removing as much of the rainfall effect on the net seepage as possible. Because of the complexity of the seepage pattern, it was decided that the correction of the measured seepages should be done to the date at which the greatest net downward seepage occurred at the control site. This would also be the measurement period farthest removed from rainfall effects. Hence, in Equation 2, the inflow from the unconsolidated sediments would be the closest to 0 for the observation period and the date corrected values would be closest to true downward seepage to the Thiensville. The time correction was treated as additive and assumed to be uniform for all sites measured on a particular date. In effect, it assumes there is no time lag of the rainfall effect with distance offshore. The correction is expressed as:

$$\text{Time correction} = q_{cm} - q_{cd}, \quad (3)$$

where:

q_{cm} = the average seepage of the two control meters (c) on the date when downward seepage is at its maximum (m); and

q_{cd} = the average seepage of the two control meters (c) on the date (d) for which the correction is being made.

All seepages used in Equation 3 have already been corrected for meter efficiency with Equation 1.

For the lake readings, q_{cm} occurred on May 27, 1992 (day 27 on Figure 9c), when a value of -5.2 ml/hour/m² was obtained. On July 22, 1992 (day 83 on Figure 9c) the average seepage recorded at the control site (q_{cd}) was -1.7 (Figure 9c); so, according to Equation 3, the correction for that date would be -3.5 ml/hour/m² to make them comparable to what would have been observed if there were no rainfall effect.

This time correction has shortcomings. It assumes that all locations will be affected by rainfall the same as at the control site and that downward seepage toward the tunnel at the control site is constant through time at a rate equal to or greater than that of May 27, 1992. Both assumptions are necessary to eliminate the observed time variations at the control site and allow comparisons throughout the summer, however, they create uncertainty as to the accuracy of the time corrected seepage. Direct quantification of this uncertainty is not possible, but it is estimated to be on the order of 25 to 30%, approximately double the error associated with the individual seepage values.

The same procedure was used to correct seepages measured on the Milwaukee River to time synchronous values. Sites A and 2 (Figure 7) were used as controls and monitored throughout the

summer of 1993. Sites 2, 7, 9, and 13 (Figure 7) were also monitored throughout the summer of 1994 to provide additional information on the temporal variation of seepages on the river.

EXCHANGES BETWEEN THE NORTHSORE TUNNEL AND LAKE MICHIGAN

After the corrections described were made to the raw observed seepages across the Lake Michigan bed they were plotted on a map and contoured (Figure 10). Measurements from two summers were combined because after time correction to a common date they were internally consistent. Forty-two seepage meter positions were used to develop Figure 10.

Longshore Distribution of Seepage

At all locations north of Milwaukee Harbor and adjacent to the Northshore Tunnel seepage was measured to be downward out of Lake Michigan and into the underlying rock units (Figure 10; Table 3). Installation of meters was not permitted in Milwaukee Harbor because their marker buoys were deemed a hazard to navigation. However, the downward seepage zone is inferred to terminate in the harbor because of the proximity to MMSD's injection wells which cause the heads in MMSD's piezometers in this area to remain above lake level.

Downward seepage persists northward to meter site 8 (Figure 10). The Northshore Tunnel is the only known groundwater sink in this area, as Fox Point, Whitefish Bay, Shorewood, Milwaukee, and the communities inland from them in the study area all use Lake Michigan as their water source. Thus the tunnel is inducing water toward it from the lake over a distance exceeding 4 km.

Outside the tunnel's influence, the observed seepages are consistent with onshore use of groundwater. Fox Point has no active wells in it, so seepage offshore is from the aquifer to the lake (positive values on Figure 10). In contrast, Bayside and Mequon residents rely on individual domestic wells for their supply. This draws aquifer heads below lake level and induces flow from the lake to the aquifer (Cherkauer and Zvibleman, 1981). With the exception of the area around meter site 8 (Figure 10), the boundaries between upward and downward seepage zones cannot be accurately located because of the distances between observation transects. Therefore, a conservative interpretation (one which minimizes seepage toward the tunnel) has been used in Figure 10.

The fact that the tunnel can induce seepage from the lake over distances of 4 km and through 10 to 20 m of relatively low conductivity glacial sediments is the direct result of the area's hydrogeology. The highly conductive Thiensville Formation (Figure 5) lies between the tunnel and the lake (Figure 11). Without the Thiensville, the tunnel's trough of depression would be very deep and steep, because it is constructed in the low conductivity Waubakee and Racine (Figure 11). The Thiensville, however, causes the trough to be very wide and relatively shallow (Figure 11), because it's able to transmit water toward the tunnel under a gentle gradient. The result is that heads which are below lake level in the Thiensville extend out under the lake, producing the downward gradient sensed by the seepage meters.

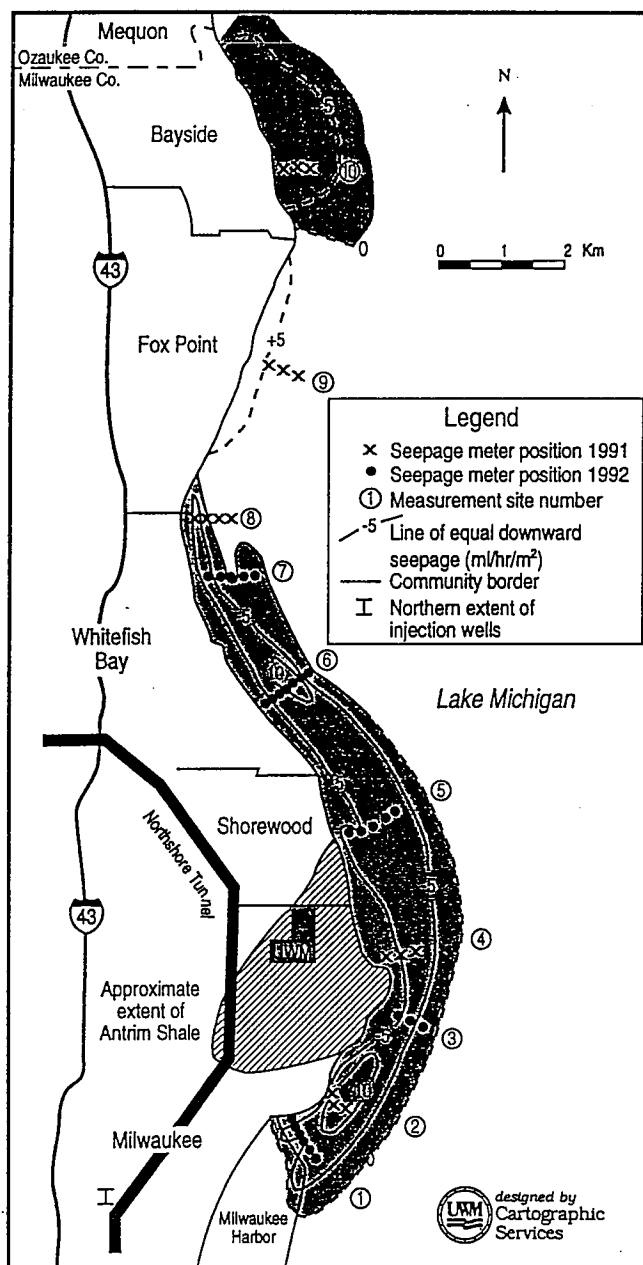


Figure 10. Composite distribution of the time-corrected seepages through the Lake Michigan bed. Individual position of meters at 10 of the 12 sites on Figure 2 are shown. Shaded offshore indicate downward seepage out of the lake. Unshaded areas show seepage into the lake. Contour interval is 5 ml/hr/m^2 with negative values indicating flow downward from the lake toward the tunnel. Of communities shown, only Bayside and Mequon use groundwater as water supply. There are no other known pumping wells in the uppermost aquifer in the area shown.

Table 3. Seepages measured along Lake Michigan.

Site†	Location	Average Seepage (ml/hr/m ²)‡	Number of Meters	Year Measured	95% Confidence Interval	
					Value	Percent
1	Breakwater	-4.1	6	1992	± 0.12	± 3.0
2	Bradford Beach	-13.6	3	1991	± 0.45	± 3.3
3	Linnwood Point	-5.2	3	1992	± 0.17	± 3.3
4	Alumni House†	-6.9	3	1991	± 0.23	± 3.3
5	Atwater Beach	-6.0	6	1992	± 0.18	± 3.0
6	Big Bay Park	-7.7	8	1992	± 0.23	± 3.0
7	Klode Park	-4.1	5	1992	± 0.12	± 3.0
8	North of Klode	-4.5	4	1991	± 0.17	± 3.7
9	Beach Drive	1.7	2	1991	± 0.09	± 5.0
10	Audubon Center	-8.0	3	1991	± 0.26	± 3.3
11	Fairy Chasm§	-4.5	2	1991	± 0.23	± 5.0
12	Virmond North	-10.4	2	1991	± 0.52	± 5.0

† Positions are shown on Figure 2.

‡ Seepages have been corrected to a synchronous date of June 5, 1992.

§ These are control sites at which numerous readings have been made.

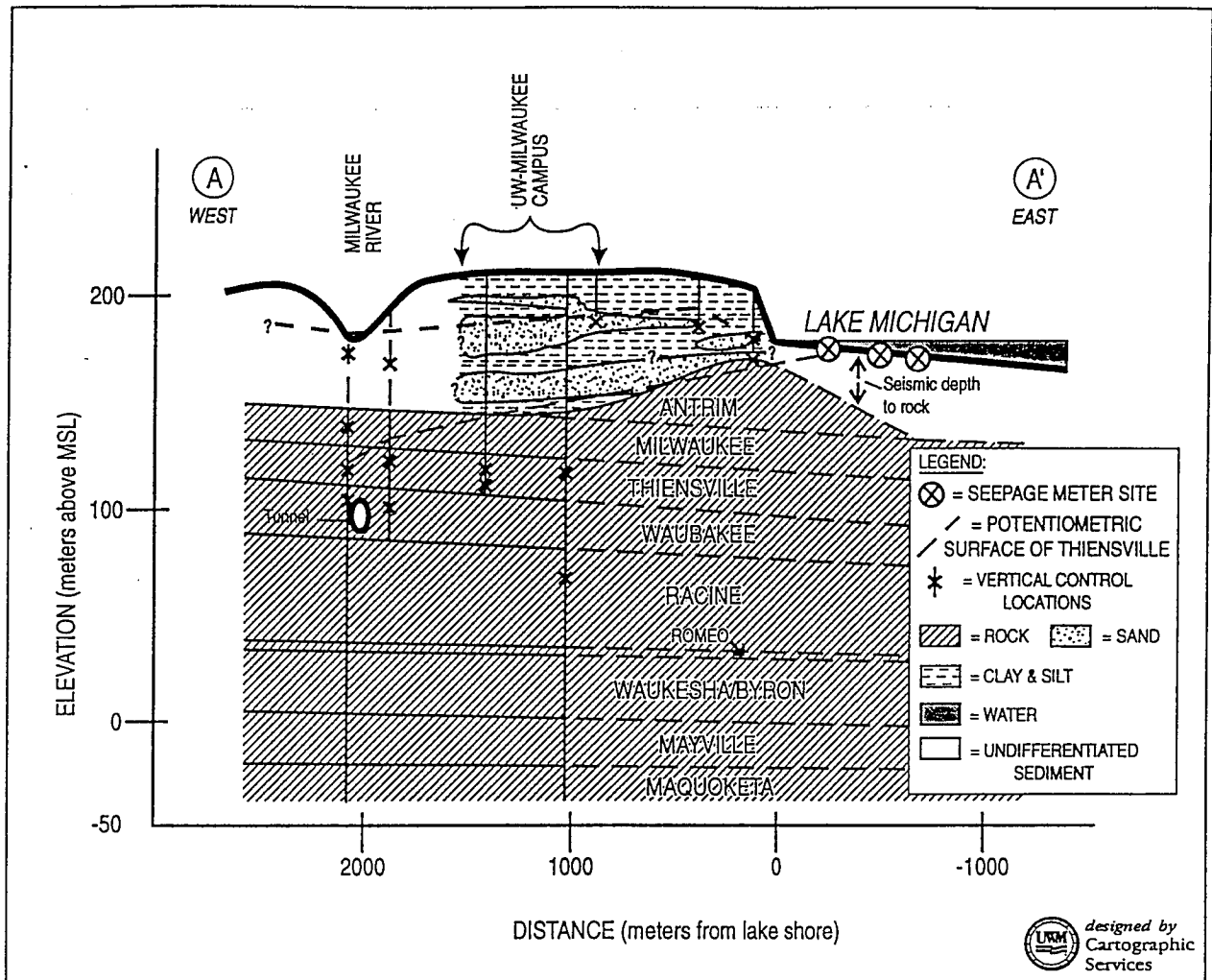


Figure 11. Hydrogeologic cross section from the Milwaukee River to Lake Michigan. The location of line A-A' is shown on Figure 2. It also runs through the University of Wisconsin-Milwaukee campus and to meter site 4 on Figure 10. Vertical lines are positions of logged cores or boring used to define geology. The xs on those lines are not positions of piezometer screens. Borings near the Milwaukee River were not logged in the unconsolidated sediments. One offshore seismic depth to rock adds to control.

Offshore Distribution of Seepage

If the stress from the tunnel and Thiensville drawdowns were the sole driving force, then seepages should be most strongly downward nearshore and decrease in magnitude away from shore because the downward gradient decreases offshore (Figure 11). However, when the observed seepages are contoured (Figure 10), the downward flux is consistently highest about 1 km offshore. The difference is the result of seepage toward the lake from the unconsolidated sediments.

The piezometers above rock at the site nearest shore in Figure 11 consistently have heads above lake level (one is shown in Figure 9b). The low conductivity of the Milwaukee Formation and the Antrim Shale, where it's present, make it easier for water in the glacial deposits to flow to the lake than downward to the tunnel. The seepage meters are integrating the two flows expressed in Equation 2. For the first km offshore, the in-seepage from the glacial deposits has a noticeable effect on the total seepage. Farther offshore, as its driving head diminishes, it's masked.

It is not known how far offshore downward seepage occurs at all locations. Only at meter sites 6 and 8 did the measurement array reach a zero seepage. (In fact, at site 8 seepages became positive farther offshore.) Hence the position of the 0 contour south of site 6 is inferred (Figure 10, dashed contour), but it's believed to be shown conservatively.

Total Flow from Lake to Tunnel

The contours on Figure 11 have been used to calculate a minimum total seepage from the lake to the tunnel. The area between two adjacent contours has been measured and multiplied by the average seepage value of the two contours. Seepage inside the closed 10 contour has been assumed to average 12 ml/hr/m². Since the seepages are fluxes, the resultant of this calculation is a discharge. Discharges were then cumulated across the zone of influence, resulting in a total value of 1,600 m³/day. It should be noted that this is a minimum value. The calculations use the plotted contours everywhere. Nearshore those contours underestimate the flux out of the lake because they also include the inward flow from the glacial deposits.

Evaluation of Monitoring Methods

Seepage meters and piezometers were used to determine the impact of the tunnel on Lake Michigan, and both had advantages and disadvantages. The seepage meters provided reliable and reproducible direct measure of flux values. They are relatively easy to install and cheap to build, meaning that they can produce many readings and define the spatial distribution of seepage. They also integrate readings over a 7- to 10-day period, resulting in a value which is not strongly influenced by short-term changes in lake or groundwater levels. On the down side, they also measure the composite flux in a complex flow system, so they were unable to distinguish seepage toward the tunnel from that toward the lake from another source.

In contrast, piezometers have the advantage that their installation provides information on geology and hydraulic conductivity in addition to heads. Their disadvantages are many, however. They are expensive to install, particularly in this case where results show that nests need to fully

penetrate all the geologic media between the stress (tunnel) and the surface water body to allow accurate calculation of fluxes. To observe the tunnel's impact in this study piezometers needed to be screened in the Thiensville or installed in the unconsolidated materials in the lakebed. The latter is prohibitively expensive and difficult to accomplish on Lake Michigan. It would require a deep sea drilling operation as well as a permanent, lighted support platform to protect them from wave action and warn boaters of their presence.

The best option in this study has been the combination of onshore piezometers with numerous seepage meters. This takes advantage of the strengths of both, but still can only measure the minimum impact of the tunnel on the lake.

EXCHANGES BETWEEN THE NORTHSORE TUNNEL AND THE MILWAUKEE RIVER

Distribution of Riverbed Seepage through Time

Seepages and heads in piezometers were measured biweekly at sites 2, 7, and 13 (Figure 7) during the summer of 1994 to examine the relationship between seepage meter and piezometer readings. Seepages were also measured at a fourth site (site 9, Figure 7) but logistics prevented installation of piezometers there. The piezometers were laid out at each site to allow measurement of horizontal and vertical hydraulic gradients in the unconsolidated sediments as close as practical to the riverbed site where the seepage meters were deployed. All piezometers were constructed on land in accordance with Wisconsin Department of Natural Resources (DNR) regulation NR140. A staff gage was established at each site and all piezometers and the staff were then surveyed to a local datum, the elevation of the top of the highest piezometer casing. Hydraulic conductivities were determined from each piezometer using baildown tests and the Hvorslev (1951) method of analysis. Information about the piezometer construction is provided in Table 4.

Plot of heads, seepages, and hydraulic gradients at the three sites with piezometers (Figures 12 to 14) reveal the changes in these parameters during the summer of 1993. The Kletsch Park site (site 13, Figure 7) was established as a control site because it is outside the influence of the tunnel. The meters could not be monitored in early July (days 65 to 80 on Figure 12) because the river stage was too high for wading. Outside that time period the two seepage meters (2 and 5 m from shore) generally varied in parallel. Despite there being no groundwater stress near the site, some negative (downward) seepages were measured, and these occurred when the river level rose faster than groundwater heads. Vertical gradients measured in the piezometer nest were almost always upward, toward the river.

The Data Management (site 2, Figure 7) and Estabrook South (site 7, Figure 7) piezometers and meters are located directly above the Northshore Tunnel. It had been anticipated that these sites would show downward seepage more frequently than Kletsch Park, but that wasn't the case (Figures 12 to 14, Table 5). The Estabrook site has more frequent negative seepage than Kletsch nearshore, but not offshore (Table 5), despite generally downward vertical gradients in the piezometers (Figure 13). The Data Management site always shows a strong downward vertical gradient in the piezometers (Figure 14), but has the least frequent downward seepages.

Table 4. Information on individual piezometers installed for this study.†

Site and Piezometer Designator	Depth of Boring (m)	Position of Screen (m BGS)	Position of Pack (m BGS)	Distances from Lake or River (m)	Dominant Lithology at Screen	Hydraulic Conductivity (cm/sec)
<u>Kletsch Park</u>						
Shallow	3.2	1.7-3.2	1.4-3.2	103	Sand & clay	6.1E-04
Middle	4.9	2.4-4.0	2.1-4.0	100	Sand & gravel	1.4E-04
Deep	4.9	3.4-4.9	3.2-4.9	101	Sand & gravel	4.8E-05
<u>Data Management</u>						
East	2.9	2.0-2.9	1.2-2.9	5	Silt & clay	9.8E-06
West	2.7	1.8-2.7	1.2-2.7	25	Silt & clay	3.9E-06
<u>Eastbrook Park North</u>						
Shallow	2.7	1.2-2.1	1.1-2.1	25	Sand & gravel	ND
Deep	2.7	1.8-2.7	1.5-2.7	25	Sand & gravel	4.4E-03
<u>Eastbrook Park South</u>						
W Shallow	4.3	2.7-4.3	2.6-4.3	56	Silty clay	1.5E-03
W deep	5.5	4.0-5.5	3.4-5.5	55	Sand & gravel with clay	1.3E-04
E deep	6.7	5.2-6.7	3.7-6.7	72	Silt & clay	2.7E-06
<u>Sabin Hall (UWM)</u>						
S shallow	13.1	11.3-12.2	10.7-12.2	NA	Gravel	1.7E-03
S deep	12.1	11.2-12.7	11.2-12.7	NA	Gravel	ND
N deep	16.6	14.9-16.6	13.9-16.6	NA	Gravel	1.9E-06
<u>Alumfin House (UWM)</u>						
Shallow	25.6	24.4-25.6	24.4-25.6	100	Clay & gravel	ND
Deep	32.0	30.5-32.0	30.5-32.0	100	Shale (?)	ND
<u>Great Lakes Research</u>						
Shallow	8.5	3.7-5.2	3.2-5.2	25	Sand & silt	ND
Middle	10.7	7.9-9.4	7.9-9.4	20	Sand & silt	ND
Deep	21.9	17.1-18.6	17.1-18.6	21	Sand & gravel	ND

†BGS = Below ground surface; ND = Not determined; NA = Not applicable.

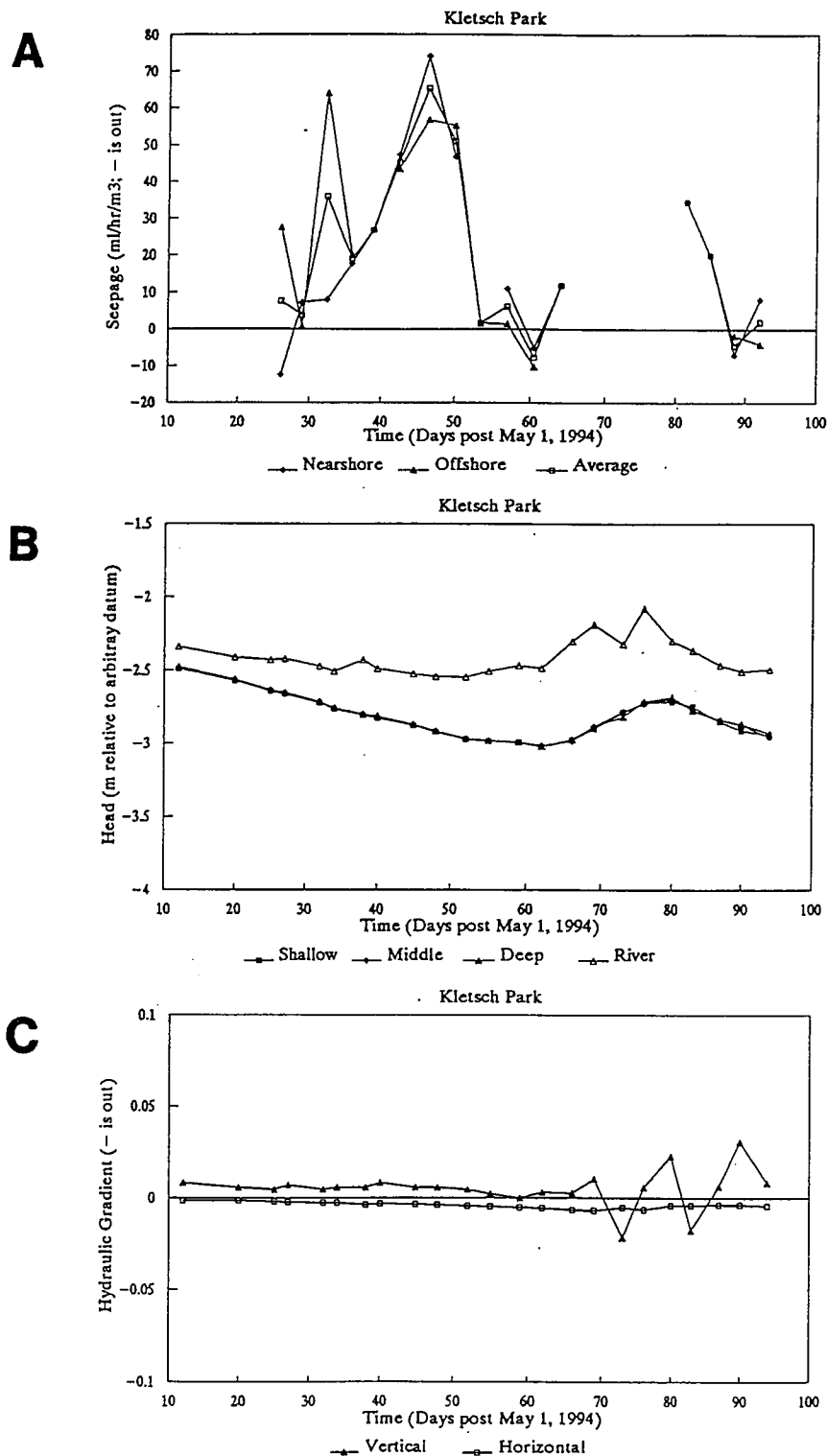


Figure 12. Seepages, heads, and hydraulic gradients at site 13, Kletsch Park, during summer 1994. Seepage at 2 m were measured twice weekly (A) except when high water or mechanical failure prevented it. At this site a single next of three piezometers is located 10 m from the seepage site. Heads in all three plus the staff gage height of the river are shown in (B) relative to arbitrary datum. Hydraulic gradients calculated from the piezometer heads are shown in (C), where a negative gradient is downward or out of the river.

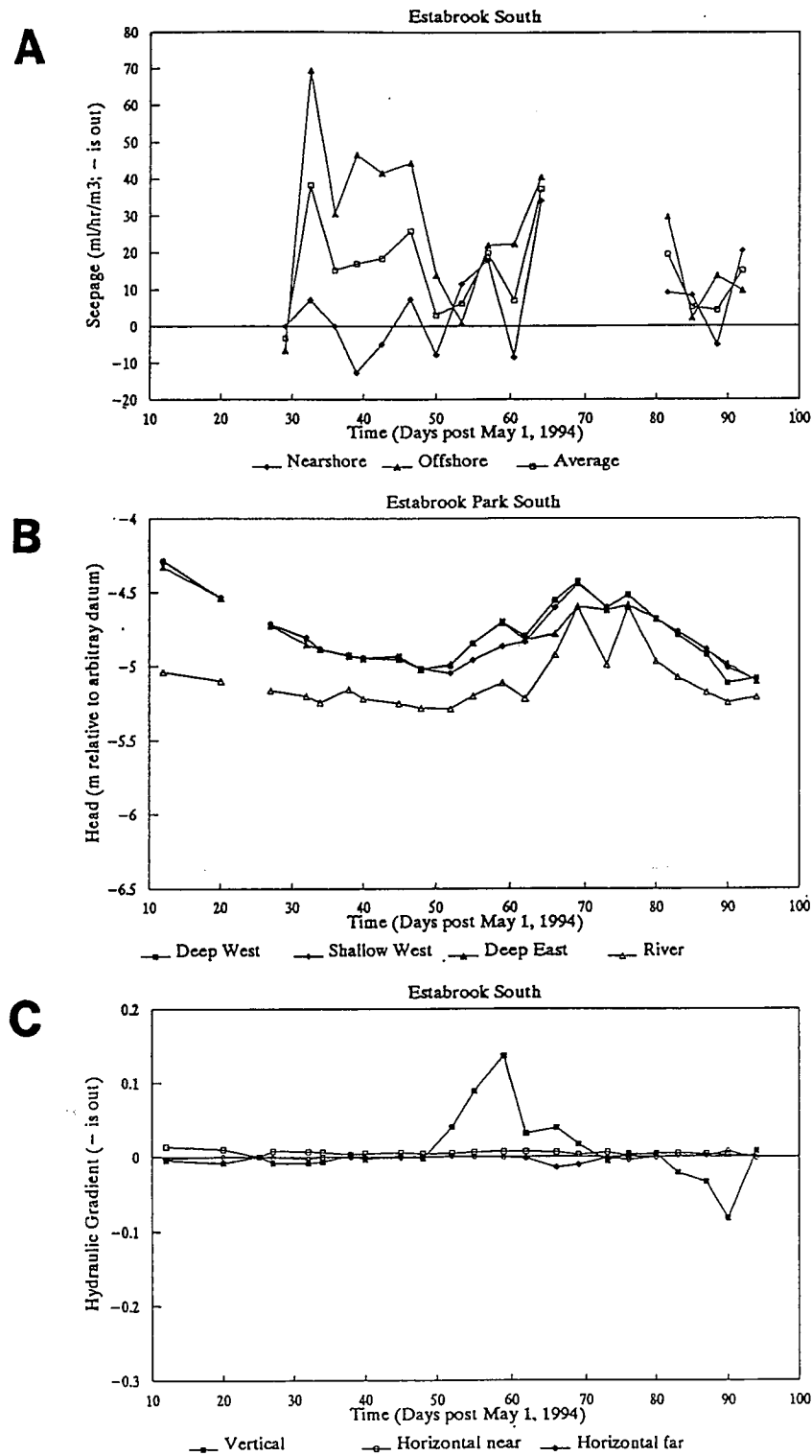


Figure 13. Seepages, heads, and hydraulic gradients at site 7, Estabrook Park South, during summer 1994. Seepages at 2 m were measured twice weekly (A) except when high water or mechanical failure prevented it. At this site a nest of two piezometers is located 55 m from the seepage site while a third is located another 15 m inland.. Heads in all three plus the staff gage height of the river are shown in (B) relative to an arbitrary datum. Hydraulic gradients calculated from the piezometer heads are shown in (C), where a negative gradient is downward or out of the river.

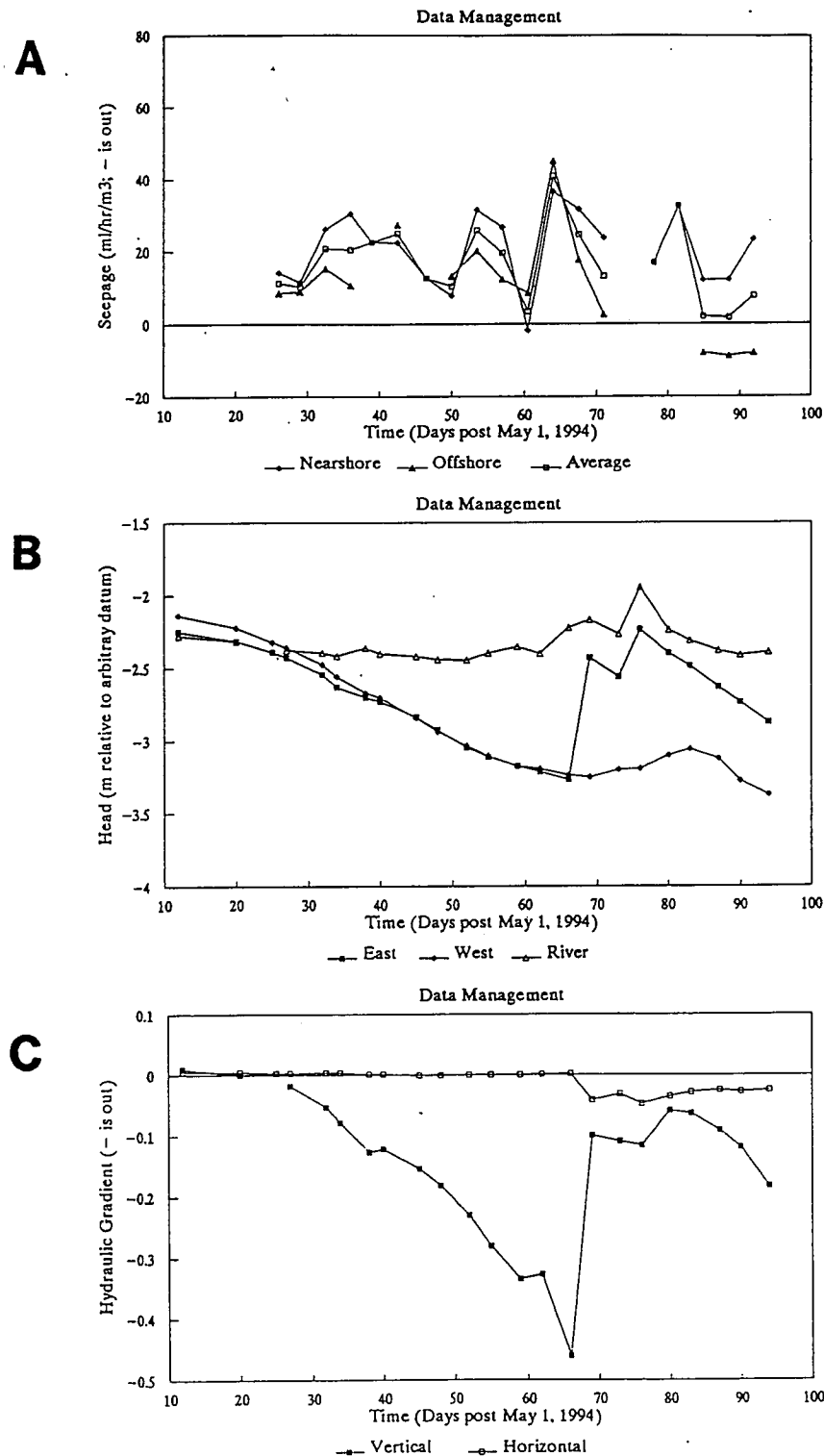


Figure 14. Seepages, heads, and hydraulic gradients at site 2, Data Management site, during summer 1994. Seepages at 2 m were measured twice weekly (A) except when high water or mechanical failure prevented it. At this site two single piezometers are located 5 and 25 m from the river bank. The close one is used in tandem with river levels to obtain a vertical gradient. Heads in both plus the staff gage height of the river are shown in (B) relative to an arbitrary datum. Hydraulic gradients calculated from the piezometer heads are shown in (C), where a negative gradient is downward or out of the river.

Table 5. Frequency of negative seepages at sites 2, 7, and 13 on the Milwaukee River.†

Site	Distance from Shore (m)		Number of Seepage Measurements		Number of Negative Seepages†		Percentage of Negative Seepages	
	Nearshore	Offshore	Nearshore	Offshore	Nearshore	Offshore	Nearshore	Offshore
Kletsch Park (13)	2	5	13	13	3	3	23	23
Data Management (2)	5	10	19	15	1	3	5	20
Estabrook South (7)	3	6	15	15	6	1	40	7

† Site locations are shown on Figure 7.

‡ Negative seepages are downward and out of the river.

The cause of the apparent anomaly is the same as that affecting the nearshore seepages in Lake Michigan, the complexity of the flow system. This becomes more apparent when seepages and hydraulic gradients are directly compared. In a simple system, they should be linearly related (Figure 15), conforming to the one dimensional form of Darcy's Law:

$$\bar{q}_v = K_v I_v, \quad (4)$$

where:

\bar{q}_v = vertical seepage (Darcian flux) [$L^3/T/L^2$];
 K_v = vertical hydraulic conductivity [L/T]; and
 I_v = vertical hydraulic gradient [L/L].

Negative gradients should cause negative seepages, and the slope of the line would be the vertical hydraulic conductivity of the river bed sediments.

At first glance, the real data don't conform to the hypothetical case. At Kletsch Park, the readings from both meters have been averaged for a given measurement period. When plotted against the measured vertical hydraulic gradient (Figure 16), they appear spread all over. The three obvious outliers on Figure 16 and one other point have a common trait; they are the last four readings taken there and occur when gradients from the piezometers are fluctuating wildly (Figure 12c). The fluctuations are in response to rainfall recharge events in late July. During May and June, limited rainfall precluded recharge as is evident from the steadily declining heads in the piezometers (Figure 12b). When just the data from the stable flow period are considered, a reasonable linear correlation is apparent (Figure 16).

The relationship in Figure 16 is still noisy, but this is because of the way the data were collected. The seepage meters are in place for 3 to 4 days and actually provide an integrated flux across the whole period. If the seepage were +3, -2, and +1 for the 3 days, the meters would record the average rate of +0.67. They gain water when the flux is positive and lose it when flux is negative. In contrast, the piezometers were read only at the beginning and end of the measurement period. The hydraulic gradients calculated at these two times were averaged and assumed to represent the average gradient for that period. For the 3-day example given previously, however, this process would miss the negative gradients altogether. That's also why the data from "unstable" periods do not adhere to the expected linear relation. Reduction of the noise in Figure 16 would require more frequent gradient measurements.

The regression line on Figure 16 also does not go through the origin. Hence, when the vertical hydraulic gradient is 0, there is still a seepage, in this case of 9 ml/hr/m² (out of the river). This is one measure of the horizontal component of the complex flow system at this site; water is flowing laterally out of the river when the vertical gradient is 0, because the river's elevation is higher than that in the piezometers (Figure 12). It's not high enough to generate a measurable downward vertical gradient, but this flow does manifest itself as a negative seepage when vertical gradients are low. When the vertical gradient is more strongly positive, inward vertical flow masks the outward horizontal flow.

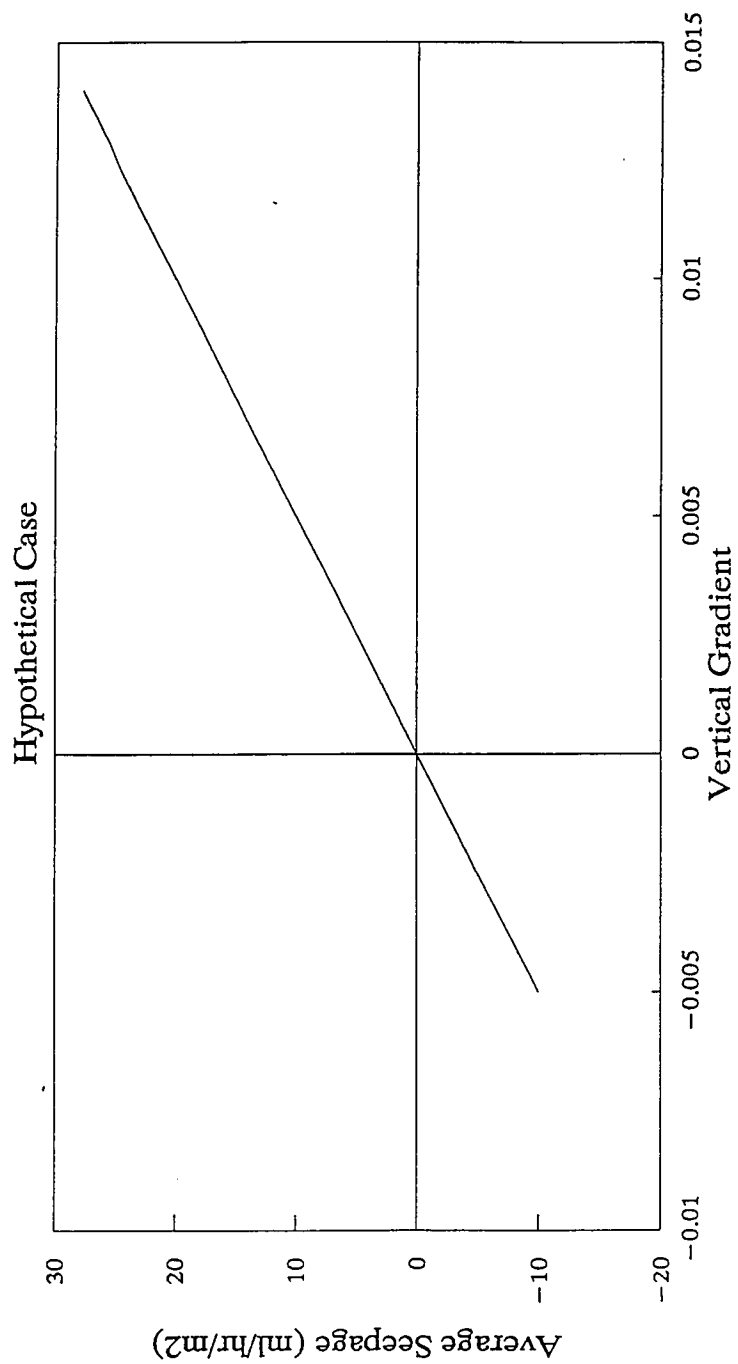


Figure 15. Hypothetical relation between hydraulic gradient and seepage at a site with simple flow. The slope of the line is hydraulic conductivity. It can be converted to units of cm/sec by dividing by $[3,600 \text{ sec/hr} \cdot (100 \text{ cm/m})^2]$.

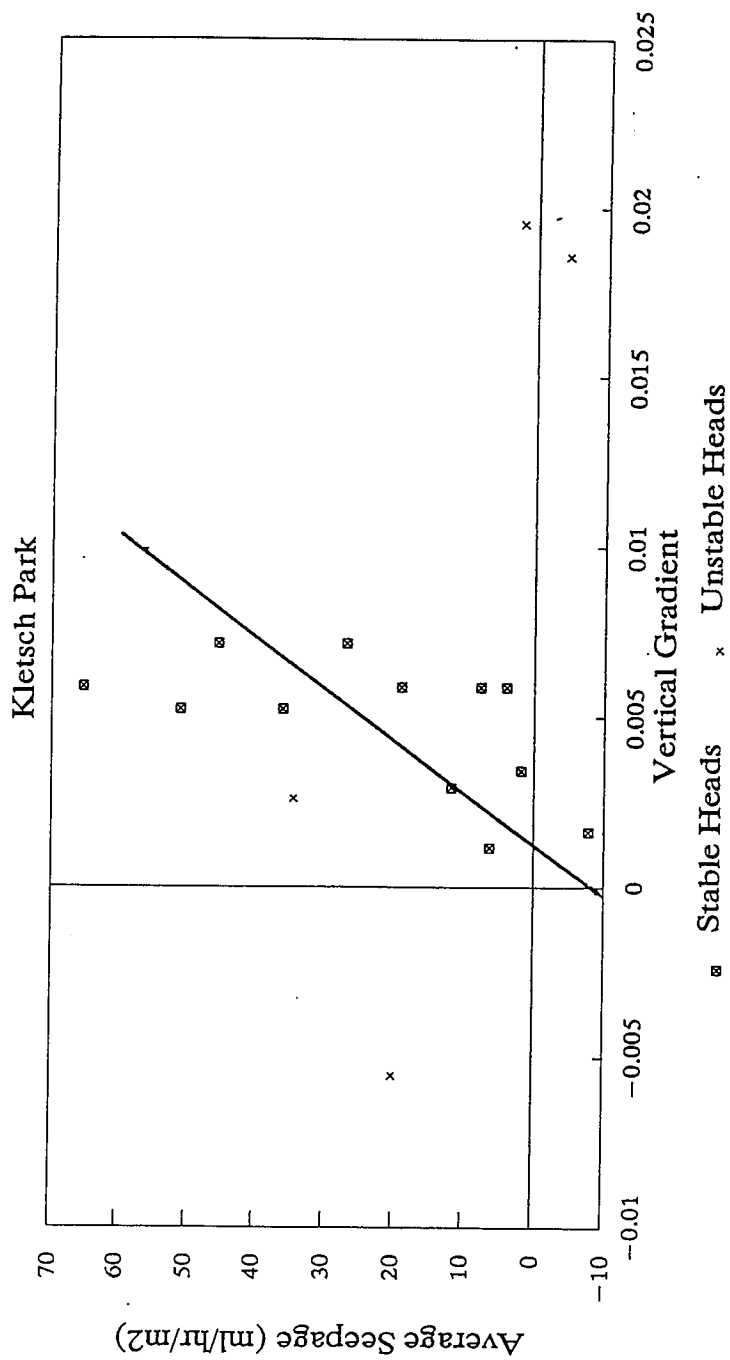


Figure 16. Relation of seepage to vertical hydraulic gradient at the Kletsch site, summer 1993. Readings from both seepage meters have been averaged for a given measurement period and compared to the average of the vertical gradients measured at the start and at the end of that period. Only points from the period of uniform flow with no recharge are plotted. The equation of the line is: $q = 6516(I) - 9$, with an $r^2 = 0.3$.

Similar patterns occur at the other two sites (Figures 17 and 18). Here only the data from stable periods are plotted. Both sites have positive intercepts, indicating the horizontal flow component is toward the river. This is logical because the river has cut 5 to 7 m below the surrounding land surface at these sites while there is virtually no relief on the banks at the Kletsch site.

The vertical hydraulic conductivities calculated from the slopes of the regression lines in Figures 16 to 18 are reasonable (Table 6). When compared with the horizontal hydraulic conductivities measured at the piezometers, they indicate that a consistent vertical anisotropy of about three occurs at all sites. This consistency indicates that the calculation procedure is valid.

The time series measurements of seepage along the river have revealed a lot about the flow system. First, as beneath Lake Michigan, the flow system has vertical and horizontal components. Where present, the tunnel induced vertical downward flow out of the river, but there is also significant, dominantly horizontal inflow from the sediments comprising the river banks. Because of the size of the lake, this latter effect is limited to nearshore and downward seepages dominate offshore. The river is never large enough for the bank effects to dissipate, even in the channel's center. Consequently, the integrated seepages measured by the meters are dominantly positive, even at the sites directly over the tunnel. Inflow from the banks generally dominates outflow toward the tunnel.

Despite that a combination of seepage meters and piezometers can determine the tunnel's effect. The seepages correlate to vertical gradients measured in the piezometer. The correlation is best when there is limited recharge occurring because the horizontal flow component and the river level are relatively constant. All attempts to correlate the observed seepages to horizontal hydraulic gradients have thusfar failed, probably indicating that the piezometers arrays were not well designed to measure horizontal flow.

Finally, a review of Figures 12 to 14 shows that two meters placed nearby at a single measurement site generally correlate quite closely, another indication that the meters are accurately sensing the real flow. Close agreement between the meters occurred 82% of the time at Kletsch, 74% at Data Management, and 60% at Estabrook South. In almost all cases, disparity between meters at a site occurred when river stage or groundwater heads were fluctuating.

DISTRIBUTION OF SEEPAGE ALONG THE RIVER CHANNEL

Seepage meters were installed at 28 sites along the Milwaukee River (18 close enough to the tunnels to be influenced by them and another 10 outside the zone of influence) to define the spatial distribution of seepage. The river lies directly over the Northshore Tunnel so the downward hydraulic gradient there should be much stronger than that beneath Lake Michigan. Furthermore, at least a part of the unconsolidated sediments beneath the river is modern alluvium (predominantly sand) and therefore the sediment column should have a greater vertical leakance ($K_v/\text{sediment thickness}$) than the combination of lacustrine and glacial sediments beneath the lake. Given these conditions, it was expected that seepage through the river bed would be strongly negative (downward) where the river lies above the tunnel and then positive (normal groundwater discharge)

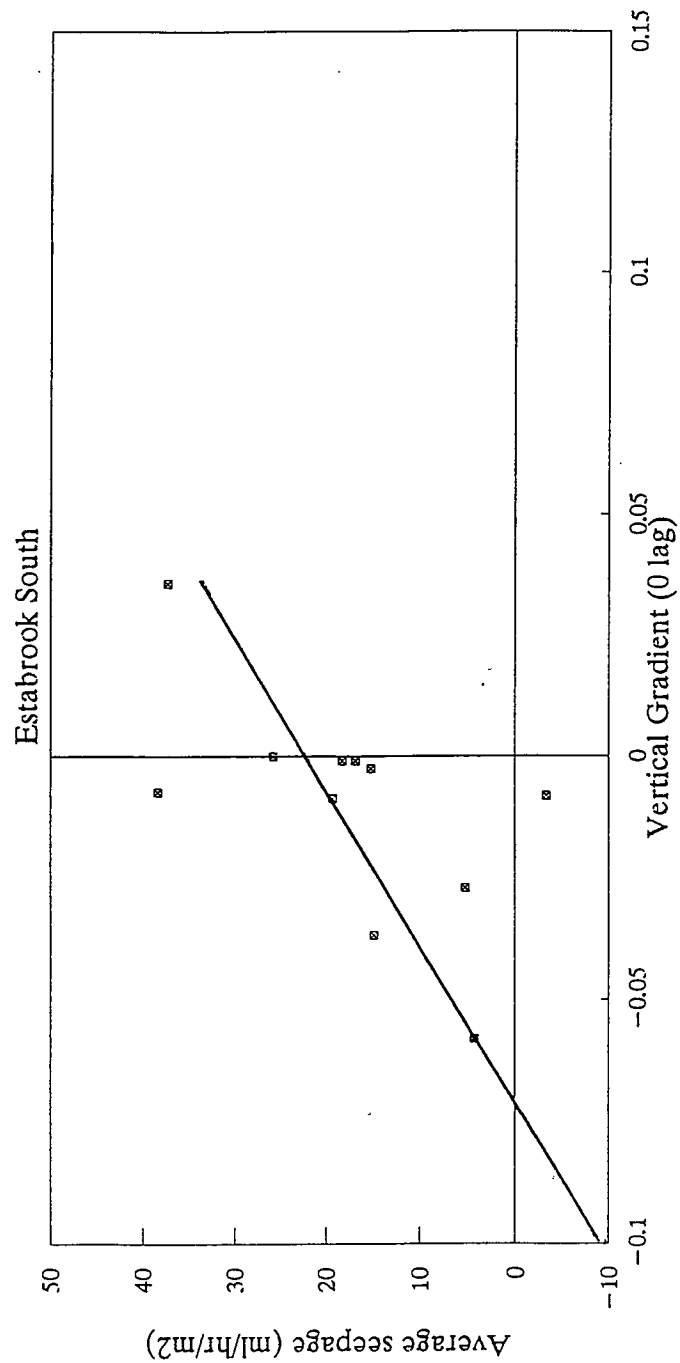


Figure 17. Relation of seepage to vertical hydraulic gradient at the Estabrook South site, summer 1993. Readings from both seepage meters have been averaged for a given measurement period and compared to the average of the vertical gradients measured at the start and end of that period. Only points from periods of stable heads are plotted. The equation of the line is: $q = 80.5(I) + 22.5$, with an $r^2 = 0.39$.

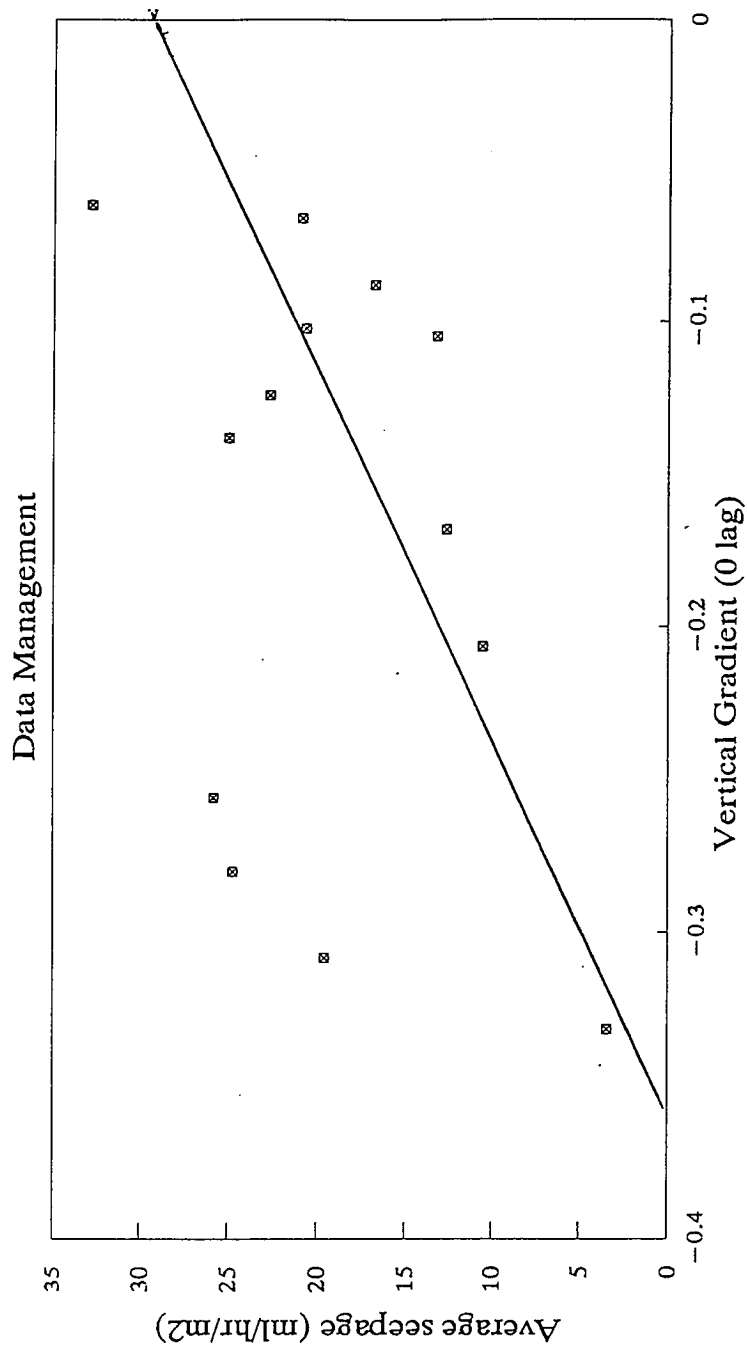


Figure 18. Relation of seepage to vertical hydraulic gradient at the Data Management site, summer 1993. Readings from both seepage meters have been averaged for a given measurement period and compared to the average of the vertical gradients measured at the start and at the end of that period. Only points from periods of stable heads are plotted. The equation of the line is: $q = 80.5(I) + 29$, with an $r^2 = 0.62$. The three points in the upper left have not been included in the regression.

Table 6. Comparison of measured and inferred hydraulic conductivities (K_s) at river seepage sites.

Site	Number of Piezometers	Geometric Mean of Horizontal K from Piezometer Tests (cm/sec) [†]	Vertical K Obtained from Seepage--Gradient Plots (cm/sec)	Vertical Anisotropy (K_h/K_v)
Kletsch Park	3	2.9E-4 [‡]	1.8E-4	1.6
Data Management	2	6.2E-6	2.2E-6	2.8
Estabrook South	3	3.5E-5 [§]	8.7E-6	3.0

[†] Raw conductivity values given in Table 4.

[‡] The deep piezometer has not been included in calculating this value as it has penetrated a different geologic unit.

[§] The two western piezometers have been averaged to represent a single point in this calculation.

upstream from the tunnel. The observed seepages (Figure 12a), however, do not follow the expected spatial pattern, just as they deviated from the expected temporal pattern.

With the exception of sites M, N, O, and P (third through sixth points from left on Figure 19a), all the sites were monitored with two or more seepage meters (Table 7). Thus, the deviation from expectations is not the result of measurement errors. In fact, six of the observation stations over the tunnels do show downward (negative) seepage (Figure 19 and Table 7) and another two are essentially at 0. But meters at 10 stations recorded upward (positive) seepage.

This dilemma was solved when the seepage distribution was compared to the underlying bedrock geology (Figure 19b) derived from MMSD cores. Where the Milwaukee Formation is present between the tunnel and the river, the observed seepages are positive at 12 of 13 stations (Figure 19). There are only four measurement stations (B and F upstream and N and M downstream) which lie over the Northshore Tunnel where the Milwaukee Formation is absent (Figure 19), and they all have downward seepages. The presence of the Milwaukee Formation does not cause upward seepage. Just as in the Lake Michigan, the exchange of groundwater with the river includes a lateral inflow component from the unconsolidated sediments and a vertical outflow component toward the tunnel. Where the Milwaukee Formation, particularly the Lindworm Member, is present, its low conductivity restricts the downward (negative) flux and allows the lateral inflow to dominate.

Because the heads, thicknesses, and hydraulic conductivities of the units between the river and tunnel are known, the downward component of seepage through the river bed can be calculated as follows:

$$q_v = K_v I_v \quad (4)$$

$$= K_v dH/B$$

$$= L_v dH \quad (5)$$

where:

- \bar{q}_v = vertical Darcian flux (seepage) (m/day);
- K_v = effective vertical hydraulic conductivity (m/day);
- I_v = vertical hydraulic gradient (m/m);
- dH = drop in head across geologic units (m);
- B = total thickness of geologic units (m); and
- L_v = vertical leakance of the units (day^{-1}).

Because flow is across a layered medium, the composite vertical leakance is calculated as:

$$L_v = \frac{1}{\sum_{i=1}^n (b_i / K_{v_i})} \quad (6)$$

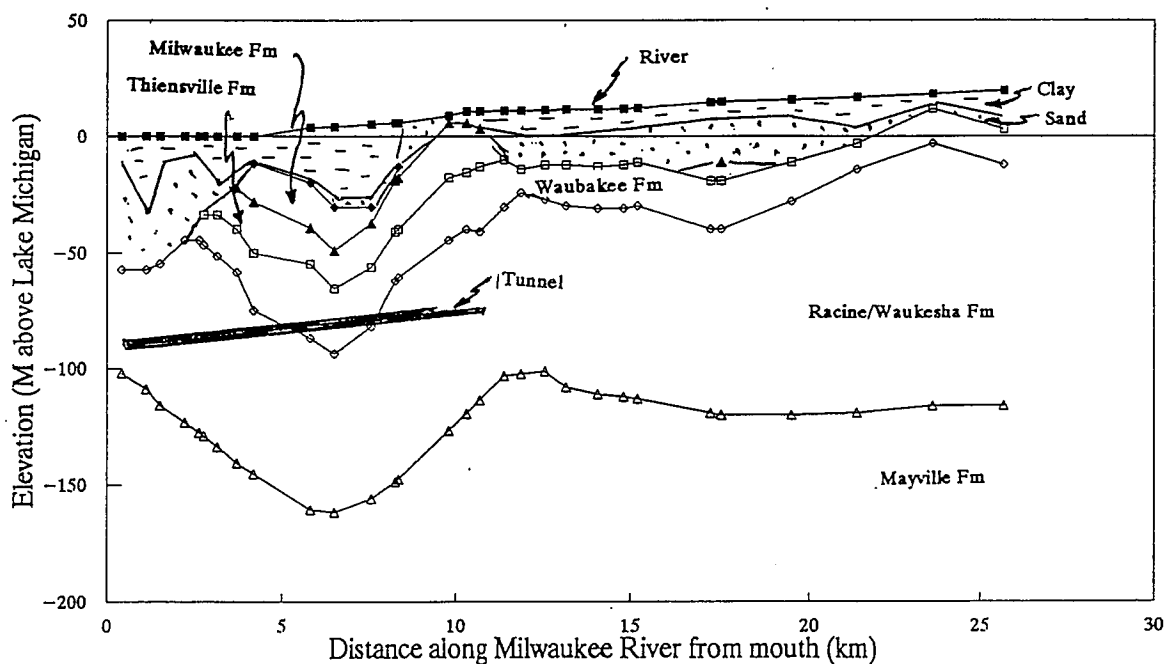
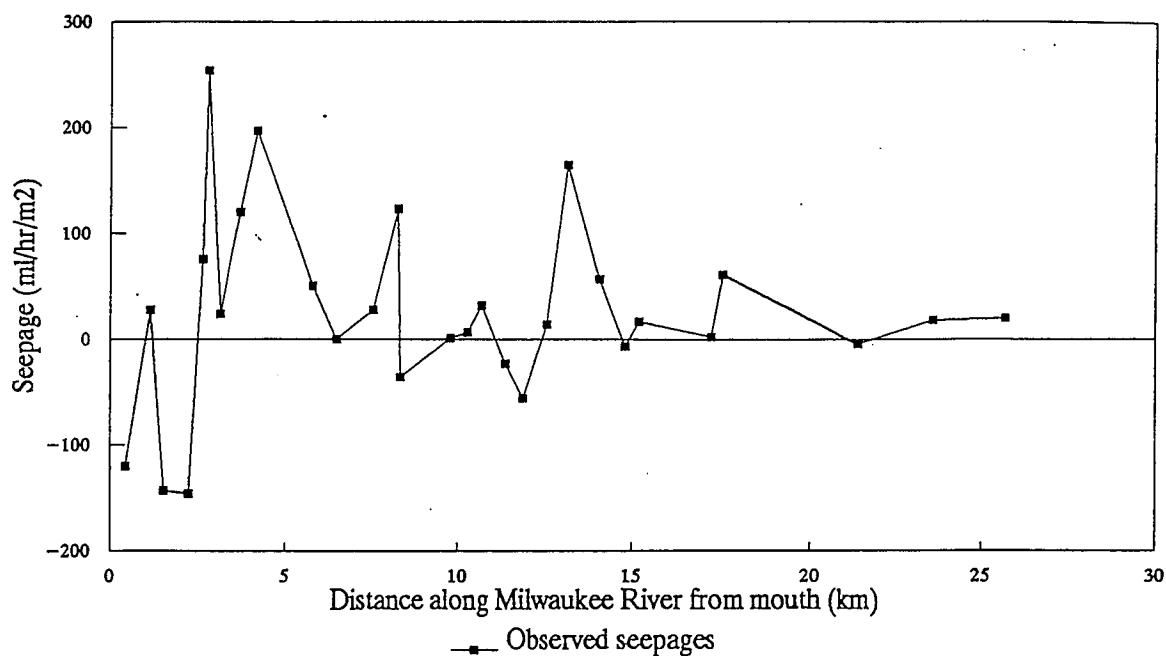


Figure 19. Comparison of observed seepages and underlying geology along the Milwaukee River. Seepages in (A) are from Table 7, averaged at a site, and then corrected to July 18, 1993. Negative seepage is downward (out of river). The geology (B) has been obtained from the Milwaukee Metropolitan Sewerage District cores along the extent of the Northshore Tunnel and from interpolation between other logged holes to the north.

Table 7. Seepages along the Milwaukee River.

Site Name†	Distance from River Mouth (km)	Average Seepage‡ (ml/hr/m²)	Number of Meters Used	95% Confidence Interval		Average Seepage§ (ml/hr/m²)
				Value	%	
Sites Above Tunnels						
K	0.43	-120	2	± 15	± 12.5	Above tunnels
L	1.13	28	2	± 3.5	± 12.5	
M	1.51	-143	1	± 70	± 49	6.6
N	2.21	-146	1	± 72	± 49	
O	2.6	76	1	± 37	± 49	
P	2.74	254	1	± 124	± 49	
Q	3.12	24	2	± 3.0	± 12.5	
R	3.72	120	2	± 15	± 12.5	
S	4.2	197	2	± 25	± 12.5	
15	6.5	0	2	± 0	± 12.5	
9	7.56	28	2	± 3.5	± 12.5	
7	8.27	123	3	± 10	± 8.5	
7A	8.35	-36	2	± 4.5	± 12.5	
2	9.8	1.3	4	±0.09	± 7	
A	10.3	6.8	4	± 0.5	± 7	
F	10.7	32	2	± 4.0	± 12.5	
B	11.4	-23	3	± 2.0	± 8.5	
CDE	11.9	-56	3	±4.8	± 8.5	
Sites Upstream from Tunnels¶						
G	12.6	14	2	± 1.8	± 12.5	Upstream from tunnels
H	13.2	165	2	± 21	± 12.5	
I	14.1	57	2	± 7.1	± 12.5	
J	14.8	-7	2	± 0.9	± 12.5	
14	15.2	17	3	± 1.4	± 8.5	44.2
13	17.2	2.3	5	± 0.2	± 7	
13A	17.5	61	3	± 5.2	± 8.5	
12	21.4	-4	3	± 0.3	± 8.5	
11	23.6	18	3	± 1.5	± 8.5	
10	25.7	20	3	±1.7	± 8.5	

† Site locations are shown on Figure 7.

‡ Seepages have been corrected to a synchronous date of July 18, 1993.

§ Site P was not included in this average because it is affected by injection.

¶ Sites 12, 11, and 10 are influenced by private wells. They are not included in average for upstream sites.

where:

- n = the number of layers or geologic units;
- b_i = thickness of the i th unit (m); and
- K_{vi} = vertical hydraulic conductivity of the i th unit (m/day).

Using the vertical anisotropies for sediments developed in Table 6 and results from the field measurements and modeling (discussed later), the vertical conductivities listed in Table 8 have been assigned for each unit. They've been combined with the thickness obtained from correlation of cores to calculate the composite vertical leakances at each seepage measurement station (Table 8). In these calculations the unconsolidated sediments have been lumped into clay and sand end members, the Milwaukee Formation has been split into its two member units, and the zone of weathered rock atop the bedrock has been included. All the other units have been treated as single entities (Table 8).

Where the Thiensville formation is present between the tunnel and river, it acts as the sink because its high horizontal conductivity transfers water from the overlying units to the tunnel. At those stations, the dH in Equation 5 is the head difference between the Thiensville and the river, and L_v is the leakance for the geologic units above the Thiensville. These heads are monitored in a series of piezometers by MMSD (Table 9). Where the Thiensville is absent (sites M, N, O, and P in Table 9) heads from the unit in which the tunnel is located are used. The L_v used then is that of all the materials between the river and the tunnel.

The actual downward flux from the river toward the tunnel was then calculated (column q_c in Table 9). When this flux is multiplied by the area of the river bed in the reach where it occurs, the end result is a projected discharge from the river to the tunnel (column Q_T , Table 9) of 536 m³/day. Based on the seepage readings, the river is actually gaining 187 m³/day of water as it flows over the Northshore Tunnel (Column Q_o , Table 9). Therefore 723 m³/day are discharging to the river from the unconsolidated sediments (Column Q_s , Table 9).

A comparison of the spatial distribution of the observed seepages and the calculated fluxes to the tunnel (Figure 20) shows that the two are similar where the Milwaukee Formation is absent. Where the Milwaukee is present, there is virtually no flux downward toward the tunnel. Where the river is deeply entrenched into the unconsolidated sediments (2.5 to 10.5 km on Figure 20), lateral inflow to the channel from sediments dominates, causing net seepages to be primarily positive.

It is unusual to have all the data necessary to calculate discharge to the tunnel as done in Table 9, so it would be useful to know if other simpler procedures produce a reasonable approximation. Three other methods were tried using just the seepage meter and shallow piezometer data, information more readily available than that from the bedrock.

- Option 1. Assume that the difference between the average seepage measured over the tunnel and that measured away from the tunnel is the result of the tunnel's influence. Then:

$$Q_T = (q_{\text{upstream}} - q_{\text{tunnel}}) A_{\text{river bed}} \quad (7)$$

Table 8. Calculation of effective vertical leakance between the river and tunnel.

Site Name†	Thickness of Hydrogeologic Units Between Tunnel and River (m)								Composite Vertical Leakance (L/sec ⁻¹)
	Sand	Clay	Weathered Rock	Lindworm	Berthelet	Thiensville	Waubakee	Racine	
M	44.0	11.0	3	0	0	0	0	6	1.3E-09
N	33.4	11.1	3	0	0	0	0	11.9	1.3E-09
O	20.5	8.8	3	0	0	0	0	15	1.5E-09
P	17.0	17.0	3	0	0	0	9.9	16.4	8.1E-10
Q	6.1	24.3	3	0	0	0.1	14.6	23	6.8E-10
R	1.4	12.6	0	0	8.2	17.6	18.7	32.2	8.5E-10
S	3.5	8.3	0	7	9.4	21.9	24.9	40	5.7E-11
15	6.9	27.7	3	6.4	9.3	16.4	28.1	0	5.8E-11
9	3.6	32.1	3	2.3	1.7	18.8	25.7	0	1.3E-10
7	5.6	16.8	2	0	0.3	22.3	21	37.1	9.6E-10
7A	19.0	0	1	0.1	3.6	22.2	21	35.9	2.3E-09
2	0	2.1	0	0	1.1	23.5	26.9	27.7	5.5E-09
A	0	4.0	0	0	0.9	21.5	24.4	25.3	3.5E-09
F	0	6.1	0	0	1.5	16.4	28.1	24.8	2.3E-09
B	14.8	6.3	2	0	0	0.1	18.4	19.5	2.5E-09
CDE	17.6	7.6	3	0	0	0.1	7	0	2.1E-09
Kv (cm/sec)	1.3E-04	1.7E-06	1.6E-04	4.2E-08	2.0E-06	1.2E-03	1.4E-05	1.4E-05	

† Site locations are shown in Figure 7.

‡ Leakance is calculated with Equation 5. Where Thiensville is present, vertical leakance is calculated only between the river the Thiensville on the assumption that water flows horizontally in the Thiensville. Thus, thicknesses in the boxed area are not used. Where the Thiensville is absent, the effects of the Waubakee and Racine are included.

Table 9. Darcian calculation of flow to the Northshore Tunnel from Milwaukee River.

Site Name†	Distance above Mouth (km)	Average Observed Seepage (ml/hr/m ²)	Composite Vertical Leackance (L/sec')	Head Difference (River to Aquifer) (m)	Seepage to Tunnel [L*H] (ml/hr/m ²)	Length of Reach (km)	Average Width of Reach (m)	Discharge to Tunnel for Reach [qc*R*W] (m ³ /day)	Discharge Observed for Reach [qo*R*W] (m ³ /day)	Discharge from Sediments for Reach [Qo - Qt] (m ³ /day)
	D	qo	L	H	qc	R	W	Qt	Qo	Qs
M	1.51	-143	1.3E-09	-29	-140.2	0.54	100	-182	-185	-3
N	2.21	-146	1.3E-09	-29	-132.8	0.545	100	-174	-191	-17
O	2.6	76	1.5E-09	-9.8	-53.7	0.265	70	-24	34	58
P	2.74	254	8.1E-10	-9.4	-27.5	0.26	50	-9	79	88
Q	3.12	24	6.8E-10	-8.2	-19.9	0.49	50	-12	14	26
R	3.72	120	8.5E-10	-6.45	-19.7	0.54	50	-13	78	91
S	4.2	197	5.7E-11	-7.4	-1.5	1.39	50	-3	329	332
15	6.5	0	5.8E-11	-12.45	-2.6	0.53	50	-2	0	2
9	7.56	28	1.3E-10	-5.61	-2.7	0.885	50	-3	30	33
7	8.27	123	9.6E-10	-3.6	-12.5	0.395	60	-7	70	77
7A	8.35	-36	2.3E-09	-3.7	-30.8	0.765	70	-40	-46	-6
2	9.8	1.3	5.5E-09	-0.6	-11.9	0.975	40	-11	1	12
A	10.3	6.8	3.5E-09	-2.5	-31.3	0.45	40	-14	3	17
F	10.7	32	2.3E-09	-0.05	-0.4	0.55	50	-0	21	21
B	11.4	-23	2.5E-09	-3.1	-28.2	0.6	80	-32	-26	6
CDE	11.9	-56	2.1E-09	-3.2	-24.3	0.25	70	-10	-24	-14
							Totals	-536	187	723

† Site locations are shown on Figure 7.

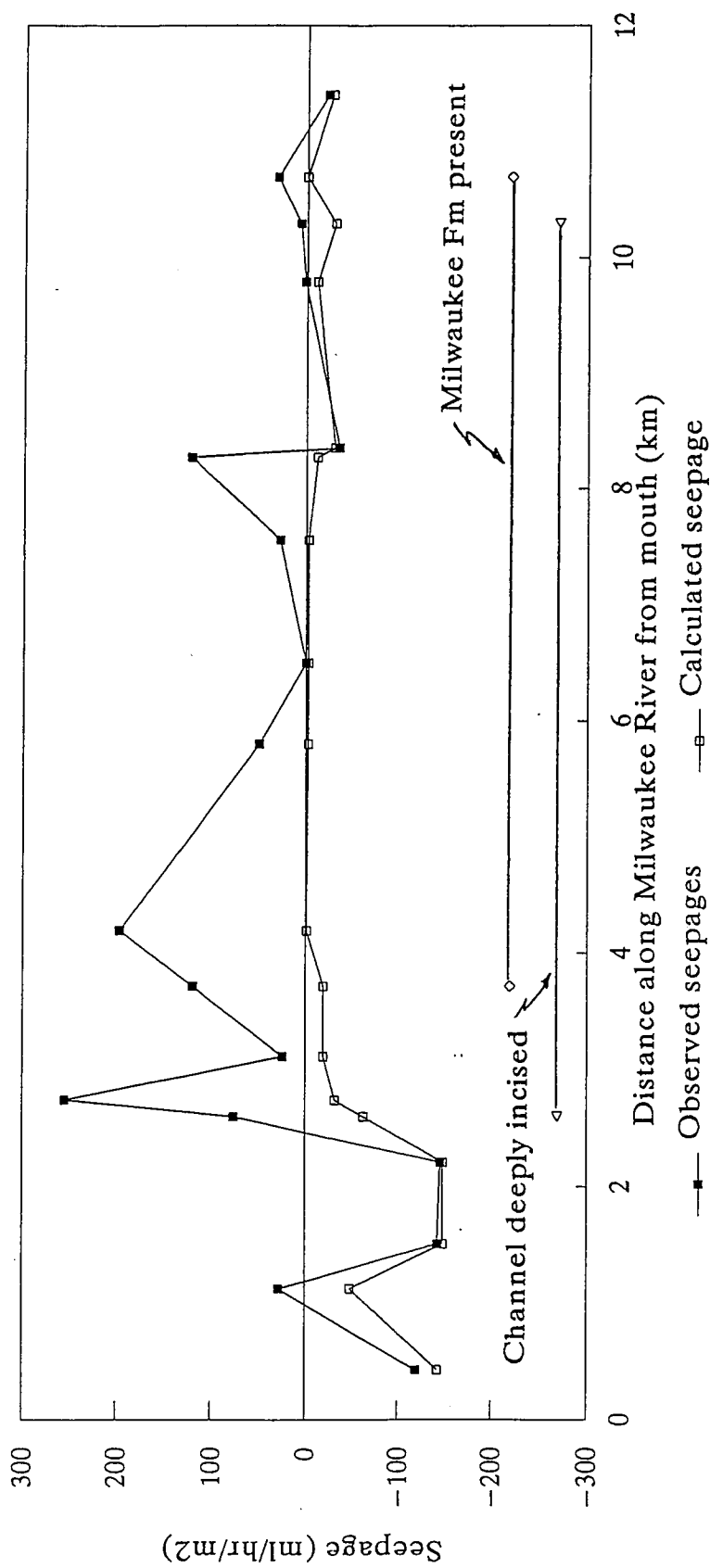


Figure 20. Comparison of calculated downward seepages with observed values from the Milwaukee River. Calculations (developed in Table 9) have been done only in the region of tunnel influence. They show the inferred seepage induced from the river by the tunnel drainage. Note the general coincidence of the two sets where the Milwaukee Formation is absent. The major exception (Site P, at 2.74 km) is adjacent to injection wells. The difference between the observed and calculated seepages is lateral influx from the river bank sediments.

- Option 2. Assume that the sites showing negative seepages over the tunnel are influenced by the tunnel and the others are not. Where downward seepage is not observed, there is no loss of river water to the tunnel. Therefore:

$$Q_T = (\bar{q}_{\text{negative}}) (A_{\text{bed in negative reaches}}). \quad (8)$$

- Option 3. Assume that along the channel half the connection between river and rock is dominated by clay (as at site 2) and the other half is dominated by sand (as at site 7). Further assume that the average hydraulic conductivities and downward gradients observed at those two sites are representative of the entire study area. Then a discharge can be calculated as:

$$Q_T = \{(K_{v \text{ clay}})(I_{v \text{ clay}}) + (K_{v \text{ sand}})(I_{v \text{ sand}})\} ((A_{\text{river bed}})/2) \quad (9)$$

In the equations above:

Q_T	= discharge from the river to the tunnel (m ³ /day);
$\bar{q}_{\text{upstream}}$	= average seepage measured upstream from tunnels (m ³ /day/m ²);
\bar{q}_{tunnel}	= average seepage measured over tunnels (m ³ /day/m ²);
$\bar{q}_{\text{negative}}$	= average negative seepage measured over tunnels (m ³ /day/m ²);
$A_{\text{river bed}}$	= total bed area in reach over tunnels (m ²);
$A_{\text{bed in negative reaches}}$	= total bed area in reaches with negative seepage over tunnels (m ²);
$K_{v \text{ clay}}$	= vertical hydraulic conductivity of clay (m/day);
$I_{v \text{ clay}}$	= average downward vertical gradient observed at Data Management site (2) (m/m).
$K_{v \text{ sand}}$	= vertical hydraulic gradient of sand (m/day); and
$I_{v \text{ sand}}$	= average downward vertical gradient at Estabrook South site (7) (m/m).

When these calculations are made (Table 10), all three optional methods produce results within 10% of the value obtained in Table 9 using site specific heads and leakances. This suggests that in the absence of heads and conductivities measured throughout the geologic sequence, the influence of the tunnel on a river can be estimated from seepage meter measurements if the meter sites are

Table 10. Comparison of methods to calculate discharge to the tunnel from the Milwaukee River.

Method Listed in Text	Procedure	Discharge (m ³ /day)	Percent Difference from Full Calculation
Full direct calculation	Equations 5, 6 and Table 9	-536	NA
Option 1	Equation 7	-505	-5.8
Option 2	Equation 8	-482	-10.0
Option 3	Equation 9	-575	+7.3

numerous and spread uniformly across the impacted area and a similar river reach outside the tunnel's influence. It would probably be even better to monitor seepage through the river bed before the system is stressed (by the tunnel) and then return to the same sites after the stress is activated. The difference between the two sets of measurements would be the result of the stress. Unfortunately, in this case, that option could not be tested because the pre-stress measurements were never made.

The comparability of the discharge to the tunnel calculated with shallow piezometer data (Option 3) to that from Table 9 is believed to be largely coincidental. More information on the spatial distribution of the unconsolidated sediments and the gradients within them would be needed for a reliable test of this method.

Evaluation of Monitoring Methods

The same advantages and disadvantages of seepage meters and piezometers, as enumerated in the discussion of Lake Michigan, exist when they're used on the river. The results in Table 10 demonstrate, however, that a dense spatial array of seepage meters can define the magnitude of the effect of a tunnel (or other similar stress presumably) as accurately as one can get from a full array of hydraulic and hydrogeologic information from borings, core, and piezometer nests. Because the meters are so much cheaper and faster to install, they should be considered the method of choice on a river.

DIGITAL MODELING

Procedures

The grid shown in Figure 21 was superimposed on the study area. The hydrogeologic system has been conceptualized as consisting of eight layers (two unconsolidated and six rock). Calibration proceeded by varying recharge, layer conductivity, lake and river bed conductances, and tunnel conductance until the model reproduced certain target values. In this case, the primary targets were these observed fluxes:

$$\begin{aligned}\text{Discharge to tunnel} &= 4,300 \text{ m}^3/\text{day}; \\ \text{Discharge to aquifer from lake} &= 1,600 \text{ m}^3/\text{day}; \text{ and} \\ \text{Net discharge between tunnel and river} &= 187 \text{ m}^3/\text{day}.\end{aligned}$$

These were treated as primary because they are integrative, covering large areas and resulting from flow through the entire system. Site-specific heads were used as secondary targets for two reasons. First, measured values in the bedrock tend to be distributed in a linear fashion right along the tunnel so they do not provide a good test of the model's general performance. Secondly, because of the strong vertical gradients caused by the tunnel, the head at a specific piezometer will depend strongly on where that piezometer is located vertically within a geologic unit. As conceptualized, the model can only calculate the average head for a layer in a node. It will, therefore, underestimate heads for piezometers at the tops of units above the tunnel and overestimate those at the bottoms.

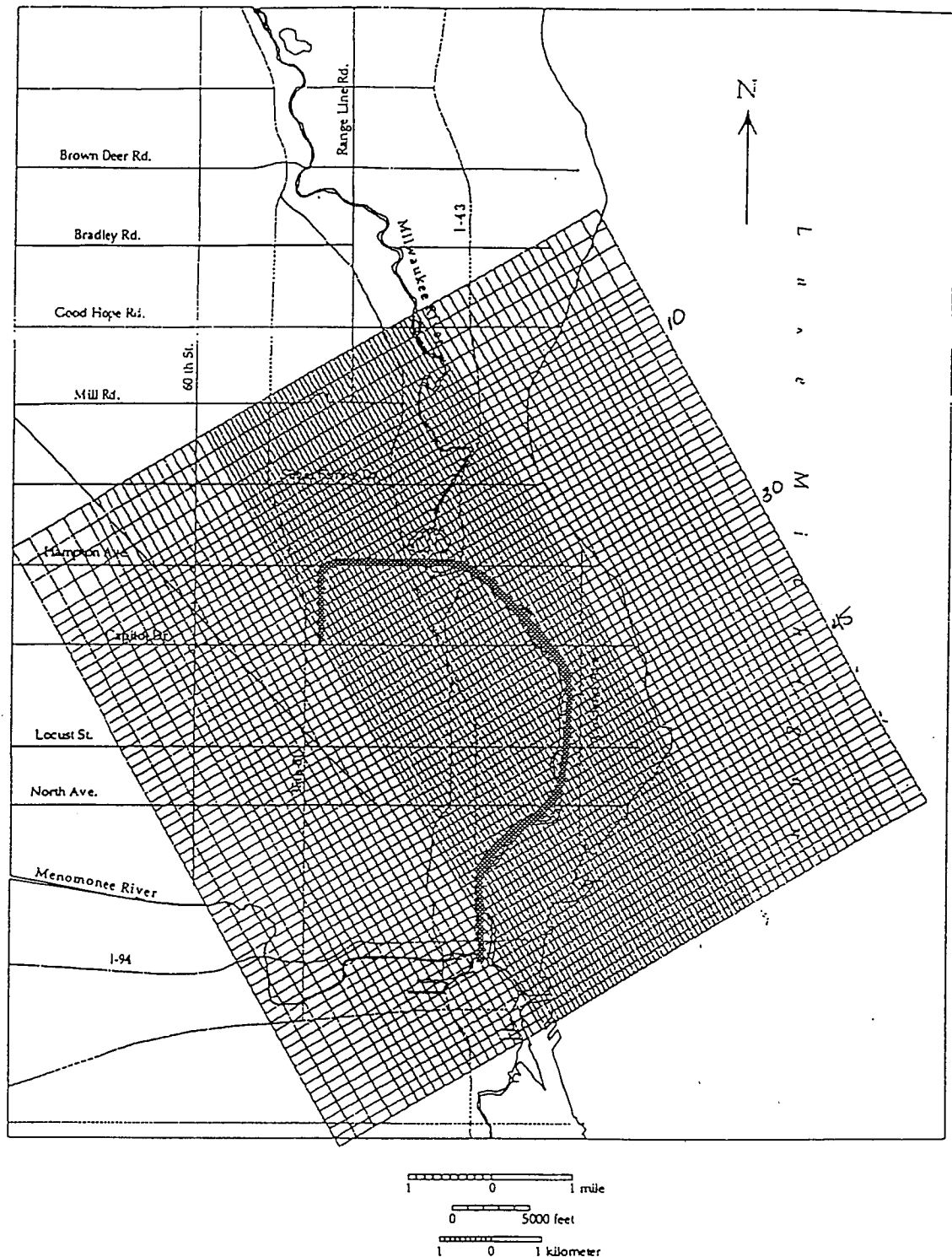


Figure 21. Location of the finite difference grid for the model. The grid's spacing is finest over the Northshore Tunnel (dark broad line). The northeast and southeast boundaries are no flow, while the northwest and southwest are specified flux and head dependent, respectively. A constant recharge is entered through the top (from Linnemanstons, 1996).

All layer and bed conductivities were treated as spatially uniform throughout most of the calibration process. Recharge was also applied uniformly. Tunnel conductance was varied spatially in response to known changes in tunnel diameter and in grout applications.

Calibrated Results

The best fit of the model to targets was obtained with a uniform recharge rate of 1 cm/year applied across layers having the hydraulic properties listed in Table 11. Target fluxes for the tunnel and river were matched very well (Table 12), but the model underestimated outflow from the lake. No reasonable combination of properties and recharge stress would reproduce the observed seepage. In fact, to obtain the 1,300 m³/day value, it was necessary to increase the vertical conductivity of the Milwaukee Formation under Lake Michigan substantially, the one deviation from uniformity of layer conductivities allowed.

Heads in bedrock (Figure 22) and the unconsolidated sediments (Figure 23) were reproduced reasonably well. When the simulated heads are plotted in cross-sectional view (Figures 24 and 25) they reveal a great deal. First, note that the tunnel's trough of depression is deep and narrow in the Waubakee/Racine Formation, but when it reaches the high conductivity Thiensville, it spreads out laterally. The gentle gradient in the Thiensville then extends the trough to the pinchout of the Thiensville to the west (the rapid rise in head at 6,000 m in Figure 24 and at 3,200 m in Figure 25) and under Lake Michigan to the east. In addition, a downward gradient exists in the units above the tunnel, but below it (Layers 6, 7, and 8) there is an upward gradient. Finally, the influence of Lake Michigan is dramatic, but that of the Milwaukee River is minor. All heads in the groundwater system converge toward the level of Lake Michigan (176.8 m) and reach it within a few km offshore (Figures 24 and 25), because the lake is such a huge water source or sink. In contrast, the river's presence is generally only observed in the topmost one or two layers (Figure 25) and then only for a few hundred meters on either side. It is completely isolated from the groundwater system below the Milwaukee Formation on Figures 24 and 25.

The offshore distribution of seepage observed in the field (Figure 10) is well-reproduced by the model at the northern and southern ends of the study area (Rows 10 and 50 on Figure 26), but the downward seepage doesn't extend as far north as observed (Row 30 should show downward seepage). Coupled with the model's underestimation of flow from the lake to the aquifer, this suggests that there is a region just offshore in Lake Michigan (from Row 15 to about Row 35) in which the connection between Lake Michigan and the aquifer is greater than simulated. This would result from the Milwaukee Formation being thinner or having a higher vertical conductivity than simulated. As mentioned previously, it has already been necessary to increase K_v offshore. All this suggests that the weakest part of the model is the distribution and K_v of the Milwaukee Formation beneath Lake Michigan.

The recharge rate in the calibrated model (1 cm/year) is considerably lower than that measured previously in Ozaukee County north of the study area. There, in southern Mequon, Cherkauer and Bacon (1978) found the rate was 6.1 cm/year. The geology of the two locations is similar, but the modeled area in this study is fully urbanized with an integrated storm drainage system. Mequon,

Table 11. Hydraulic conductivities used for the Northshore Tunnel simulation (from Linnemanstons, 1996).

Model Layer Number	Hydrostratigraphic Unit	Horizontal Hydraulic Conductivity (cm/sec)	Vertical Hydraulic Conductivity (cm/sec)	Vertical Anisotropy (Kh/Kv)
1	Glacial sediments	1.00E-05	4.00E-07	25
2	Weathered zone/New Berlin Formation	1.23E-04	4.29E-06	29
3	Milwaukee Formation	8.88E-06	2.22E-07	40
4	Thiensville Formation	1.25E-02	1.25E-03	10
5	Waubakee/Racine Formation	1.44E-05	1.44E-05	1
6	Romeo beds	1.64E-03	1.64E-05	1
7	Manistique Formation	1.18E-05	1.18E-05	1
8	Mayville Formation	1.25E-04	1.25E-04	1

Table 12. Calibration targets for the finite difference model.

Target	Observed Value (m ³ /day)	Calibrated Model Result (m ³ /day)
Primary		
Discharge to tunnel	4,300	4,250
Seepage from lake to aquifer	1,600	1,300
Net seepage between river and aquifer	190	198
Secondary		
Heads at specific locations	See Figures 22 and 23	

Head correlation

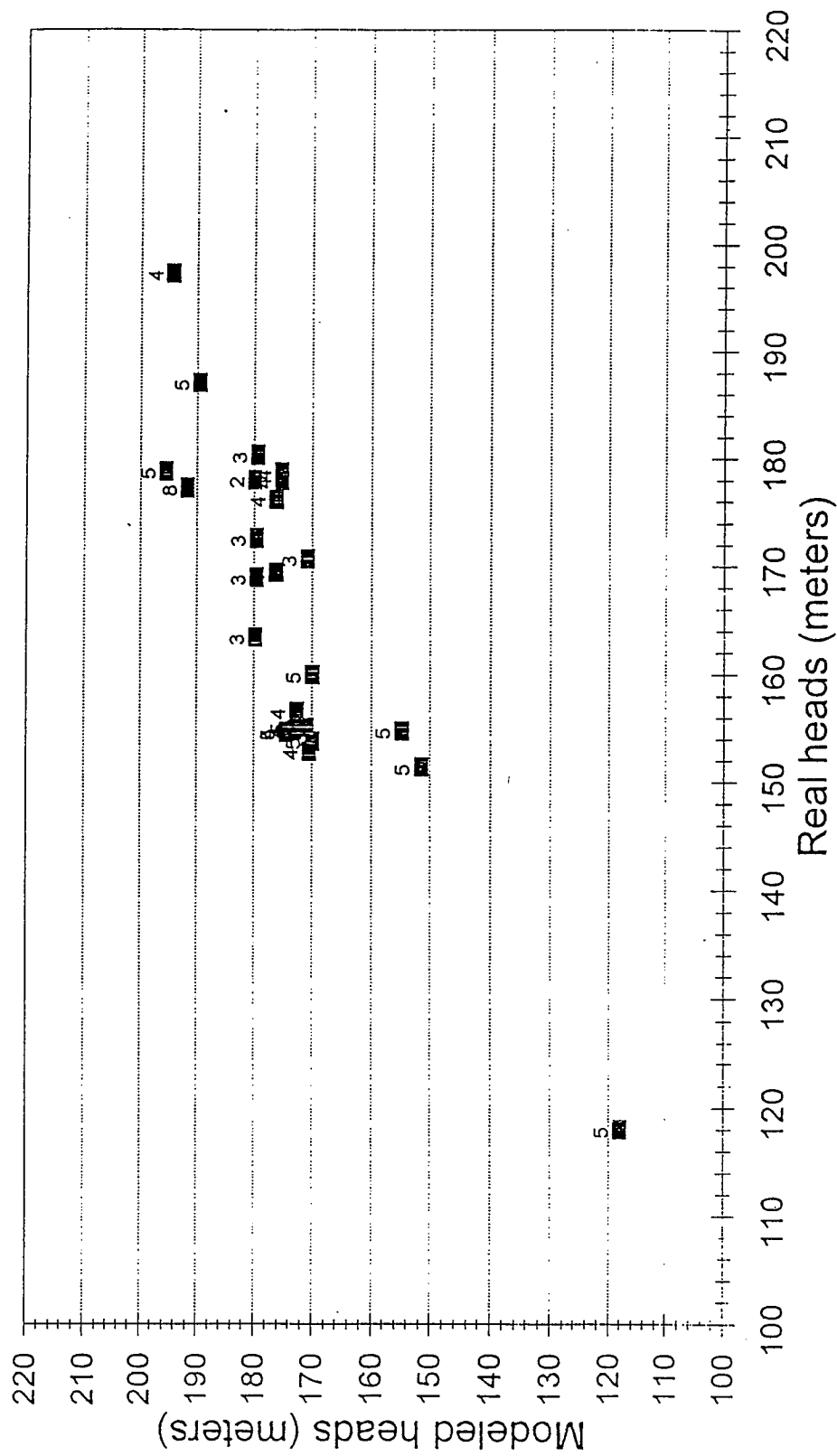


Figure 22. Comparison of observed and modeled heads in bedrock. Numbers on graph are the layer in which the piezometer is screened. Scatter is due to the fact that strong vertical gradients in the real units cannot be reproduced by the model which simulates each unit as a single layer.

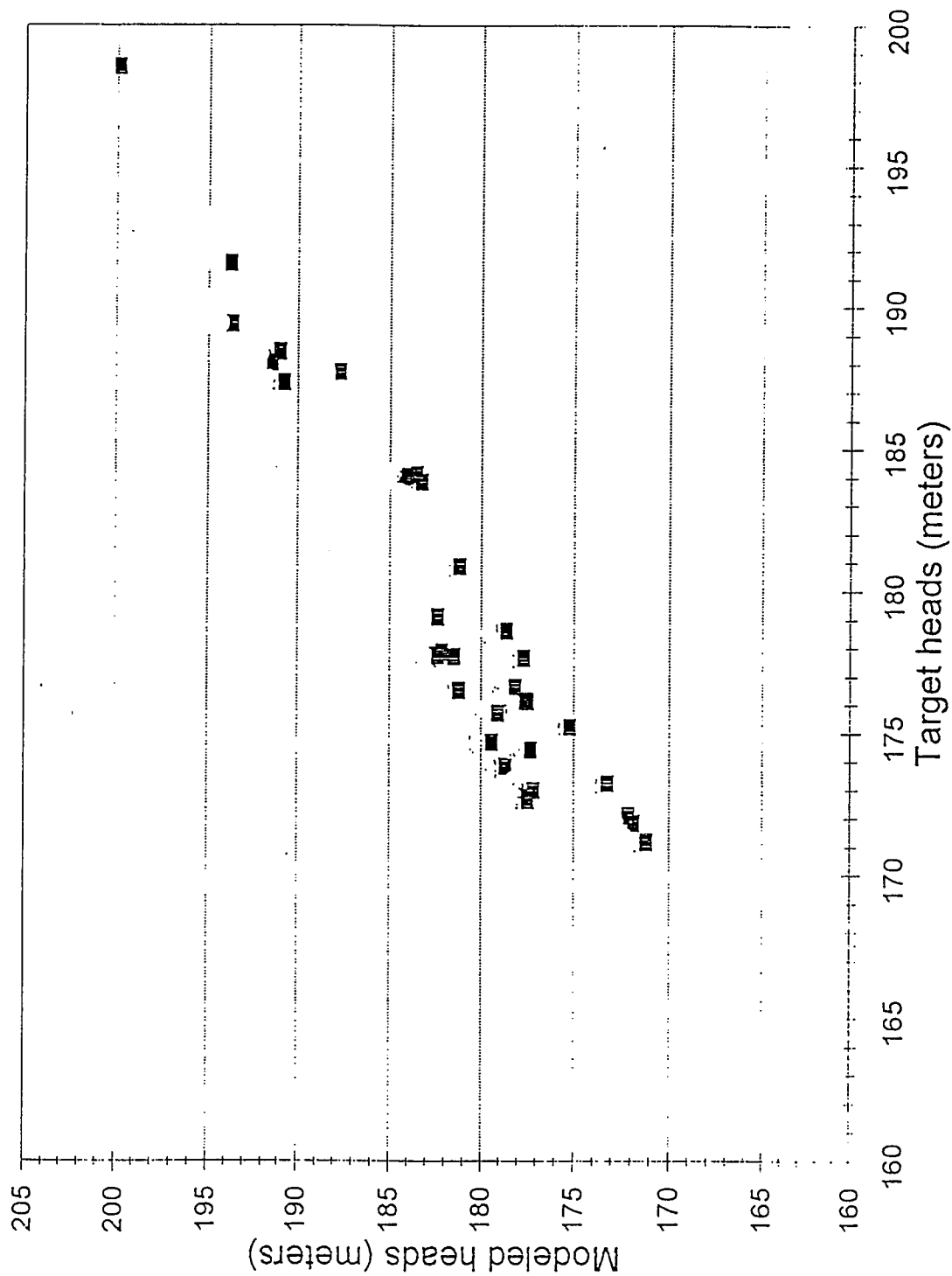


Figure 23. Comparison of observed and modeled heads in unconsolidated sediments. Scatter is due to the fact that strong vertical gradients in the real units cannot be reproduced by the model which simulates each unit as a single layer.

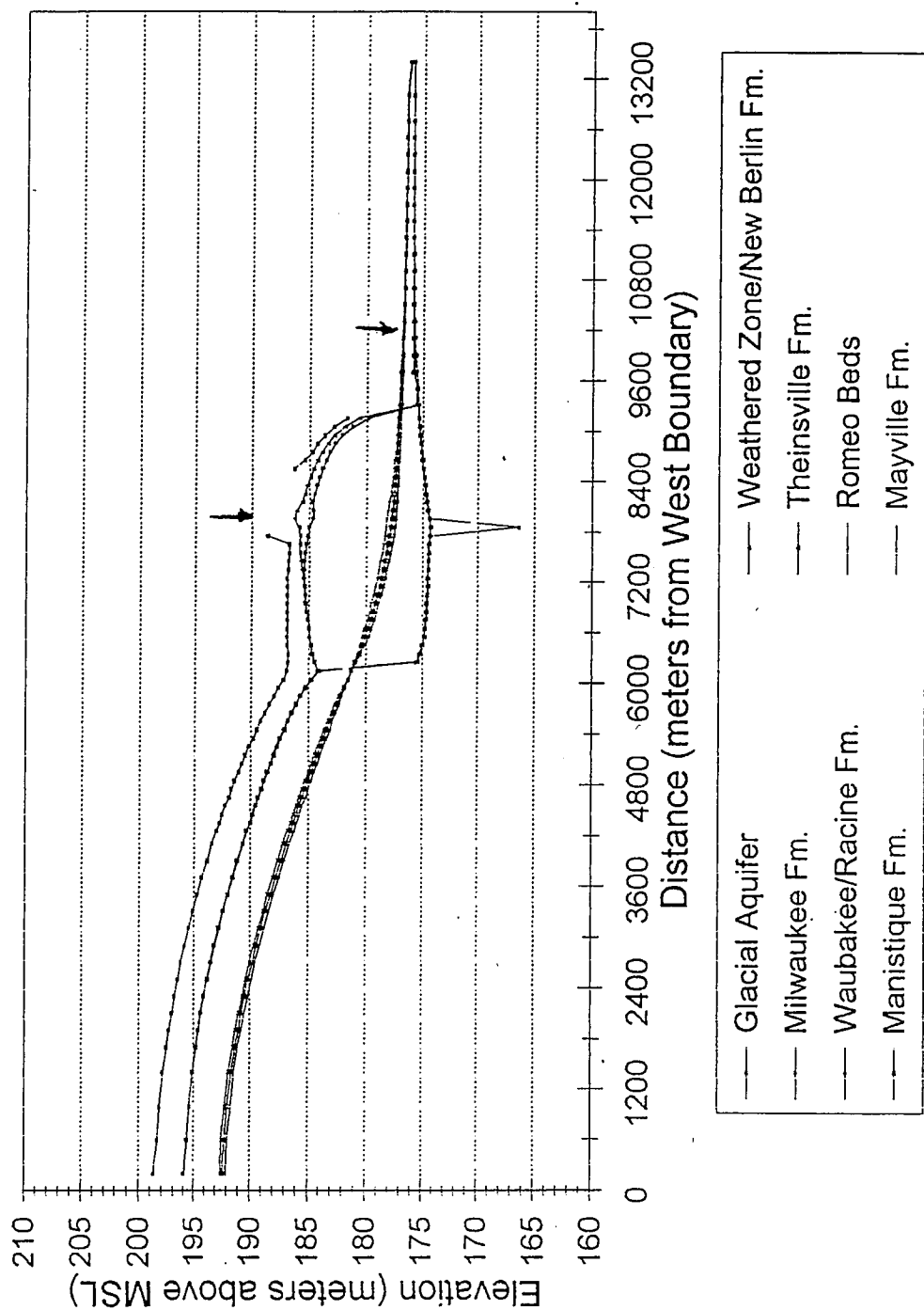


Figure 24. Distribution of simulated heads along Row 30 in calibrated model. The tunnel is the trough at 7,800 m. Heads in a layer are discontinuous where water level drops below base of layer. Vertical arrows point to positions of Milwaukee River (left) and Lake Michigan shore (right). Row 30 is marked on Figure 21. Lake Michigan is on the figure's east side and has a head of 176.8.

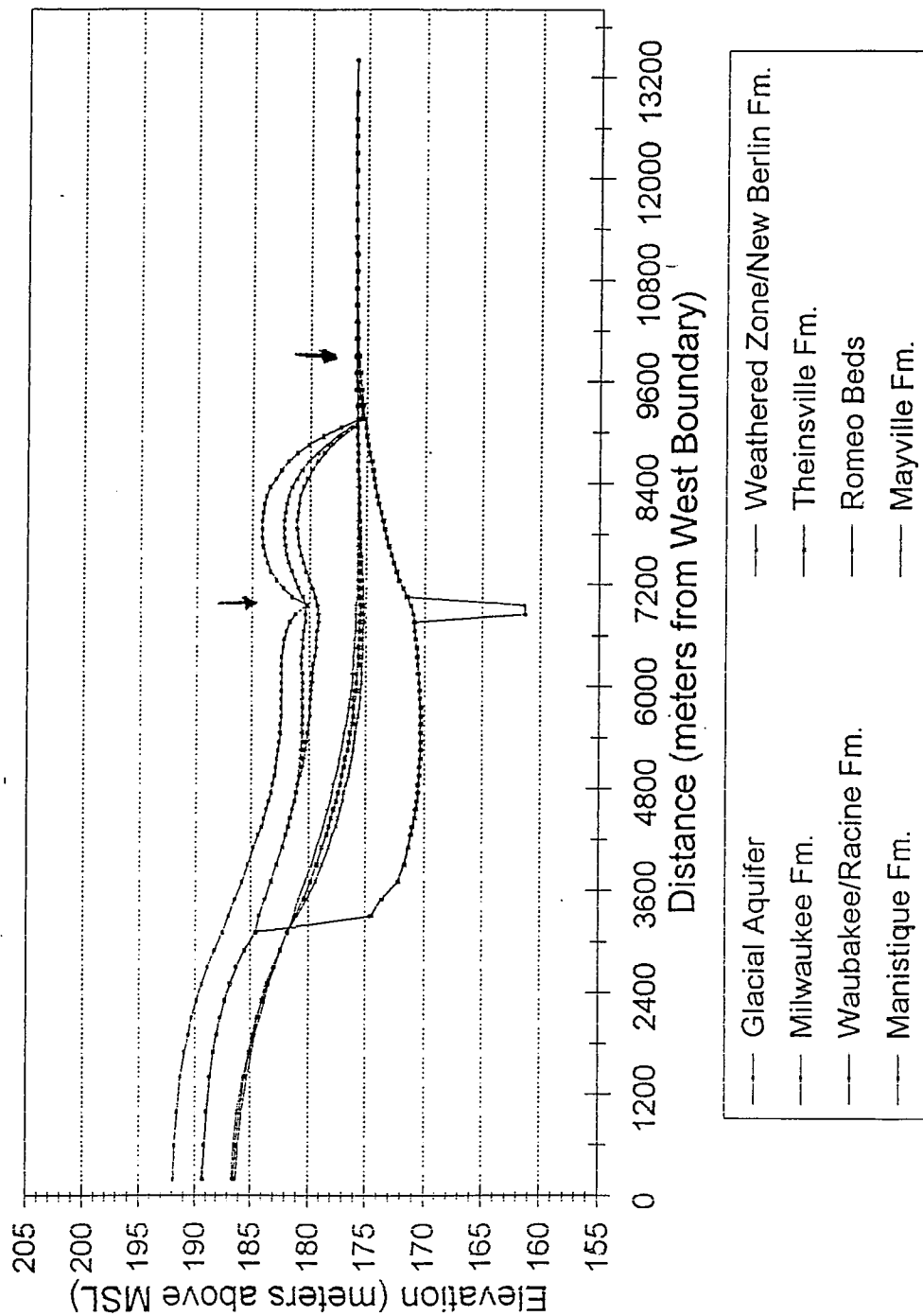


Figure 25. Distribution of simulated heads along Row 45 in calibrated model. The tunnel is the trough at 7,800 m. Heads in a layer are discontinuous where water level drops below base of layer. Vertical arrows point to positions of Milwaukee River (left) and Lake Michigan shore (right). Row 30 is marked on Figure 21. Lake Michigan is on the figure's east side and has a head of 176.8.

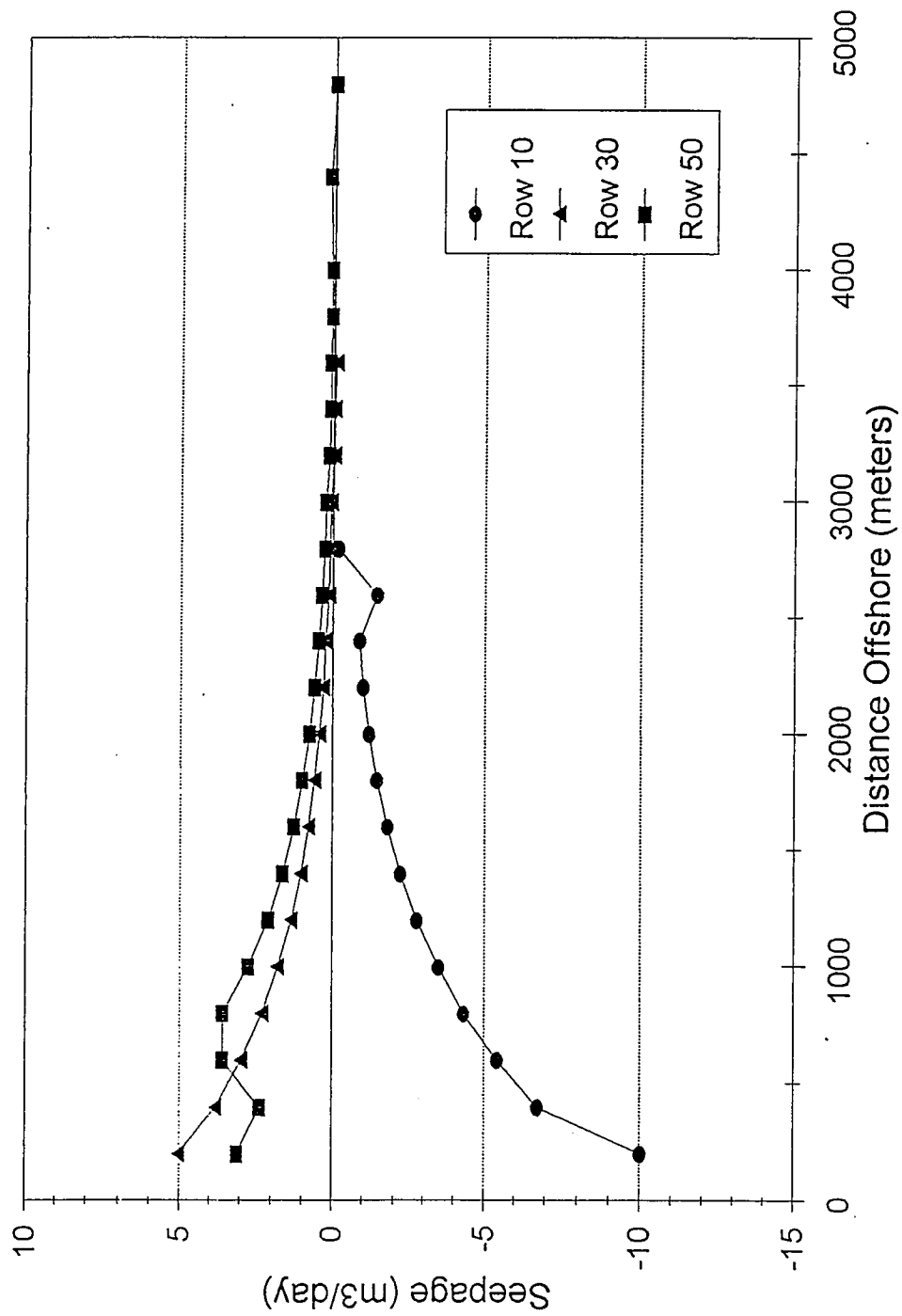


Figure 26. Offshore distribution of seepage as simulated by flow model. Position of lines is shown on Figure 21.

in contrast, has no storm sewer system, so the lower recharge value is reasonable and attributable to the study area's urbanization.

In summary, the model has been able to reasonably reproduce all the observed aspects of the groundwater/surface water/tunnel interaction but two. Apparently, the Milwaukee Formation does not have properties beneath Lake Michigan that are simple extrapolations from onshore. In addition, the vertical anisotropy obtained from comparing seepage meter and piezometer readings (Table 6) tends to be an underestimate; it tends to overestimate the K_v of the units (compared to the values needed to calibrate the model, Table 11). Otherwise, the model has confirmed the field observations about extent and magnitude of impact.

CONCLUSIONS

The extent and magnitude of the impact of MMSD's tunnels on surface water bodies was defined to evaluate the hydrogeological factors controlling those impacts were defined and a protocol to use in monitoring other stressed systems was developed. Logistical and practical constraints required that efforts be concentrated exclusively on the Northshore Tunnel and its impacts on Lake Michigan and the Milwaukee River. The reduced scope of the study, however, still allowed completion of the objectives.

EXTENT AND MAGNITUDE OF IMPACTS

The Northshore Tunnel induced recharge of at least 1,600 m³/day from Lake Michigan and 534 m³/day from the Milwaukee River in 1992 and 1993, respectively. This compares to a total groundwater drainage to the tunnel (before the tunnel was activated) in early 1993 of about 4,300 m³/day. Caution should be exercised in combining the two induced recharges because they were measured at different times during a period when heads were rising in the aquifer system. It is likely that less water than reported was induced from the lake in 1993 and more was induced from the river in 1992, but no attempt has been made to estimate those values.

The impact of the tunnel was observed (as negative seepages out of Lake Michigan) as far as 4 km from the tunnel. In contrast, negative seepages in the river were observed no more than 0.5 km upstream from the tunnel. Based on field observations and modeling results, it is likely that the tunnel's influence is felt up to 2 km upstream. The difference between the extent on the lake and river is largely the result of the local hydrogeology.

HYDROGEOLOGIC CONTROLS ON THE TUNNEL'S INFLUENCE

In both surface water bodies, the flow through the bed in the area influenced by the tunnel is a combination of vertical flow downward toward the bedrock system and the tunnel and lateral (mostly horizontal) inflow from unconsolidated sediments. In short,

$$\begin{aligned} q_{\text{net}} &= q_i + q_u \\ &= L (dH) + K_e I_e, \end{aligned} \tag{10}$$

where:

- q = flux through a unit area of river or lake bed (L³/T/L²);
- q_{net}, q_i and q_u = net flux, flux induced toward the tunnel and effective flux from the unconsolidated sediments, respectively;
- L = vertical leakance of materials between the surface water and the stress (1/T);
- dH = the driving head or the head difference between the surface water and the stressed unit (L);
- K_e = the effective hydraulic conductivity of the sediments (L/T); and

I_e = the effective hydraulic gradient. in the sediments (L/L).

In the area studied, leakance (L in Eq. 10) is controlled by low conductivity layers in the geologic media, the driving head difference (dH) is generated by the tunnel and redistributed throughout the geologic section by high conductivity layers, and the effective gradient (I_e) is controlled by the height of the water body's banks and the proximity of the measurement site to them.

More specifically, the tunnel is constructed in the Waubeka and Racine formations, low conductivity layers of the Silurian/unconsolidated aquifer. Within these layers a narrow deep trough of depression forms over the tunnel. If conditions were homogeneous, this would restrict the tunnel's influence to a narrow area at the ground surface. However, in much of the study area they are overlain by the Thiensville Formation, a very conductive layer. This causes the trough to widen significantly, extending detectable dHs up to 4 km from the tunnel. It also reduces dH directly above the tunnel (and thus immediately under the Milwaukee River), in part explaining why downward seepages are less prevalent there than under Lake Michigan. Finally, the Thiensville essentially pinches out upstream from the tunnel under the river, causing the shorter zone of influence on the river than on the lake.

The effect of the hydrogeology on vertical leakance is best demonstrated by the Milwaukee Formation under the river. Where this relatively low conductivity unit is present between the river and the Thiensville, there is no observed downward seepage and calculations indicate that the river is essentially isolated from the tunnel. Where the Milwaukee Formation is absent, downward seepage occurs and can be observed in the field.

Finally, if the lateral influx term in Eq. 10 is bigger than the seepage induced downward, net seepage will be positive (upward). This masking of the downward flux is greatest nearshore or where the river bank or lake bluff is high, allowing groundwater heads to be higher than the surface water. This effect is most prevalent on the river because of its narrow width.

To fully understand the impact of groundwater stress on surface water bodies the local hydrogeology must be known. It is particularly important to delineate the extent of materials of extreme (high or low) hydraulic conductivity and to measure the K_v of low conductivity materials and K_h of high conductivity materials.

OVERALL ASSESSMENT OF MONITORING METHODS

Seepage meters and piezometers were used to assess the tunnel impacts. Based on their performance, it is possible to summarize their advantages and disadvantages (Table 13). Neither has clear superiority, and the best results stem from using both in tandem. Piezometers constructed in nests allow measurement of the full vertical distribution of heads and hydraulic conductivities near a water body. Seepage meters allow for collection of a dense spatial or temporal distribution of fluxes for a direct measure of outseepage caused by groundwater stresses. The piezometers can also serve as useful backup to the meters during floods. They must be read frequently (probably daily) for this purpose. Finally, this study has demonstrated that repeated, frequent measurements of

Table 13. Relative advantages and disadvantages of monitoring methods.

Monitoring Method	Advantages	Disadvantages
Seepage meters	<ul style="list-style-type: none"> . Quick installation . Cheap to construct . Replicable . Integrate conditions over installation period . Work in all quiet water conditions . Sensitive to underlying geologic conditions . Measure flux directly 	<ul style="list-style-type: none"> . Cannot operate on rock beds . Difficult to operate in deep water with strong current . Not operable in river floods . Cannot be sampled for water quality, head or hydraulic conductivity
Piezometers	<ul style="list-style-type: none"> . Provide direct measure of groundwater head . Allow measurement of horizontal hydraulic conductivity . Installation allows sampling of geologic materials . A standard measurement technique . Complete nested set between water body and stress provides full assessment 	<ul style="list-style-type: none"> . Installation is costly and slow . Cannot measure vertical hydraulic conductivity needed to calculate flux . Installation in water body is difficult <ul style="list-style-type: none"> Offshore drilling equipment is uncommon Sealing to prevent surface water incursion is difficult Access to measure heads is difficult . Non-integrating over time -- therefore, must be monitored frequently

seepage meters and adjacent piezometer nests allows calculation of an effective vertical hydraulic conductivity, something unattainable from either method individually.

RECOMMENDATIONS

Based on this study, it is possible to present a protocol which should maximize our ability to monitor the impact of groundwater stresses on surface water systems. First, collect all available information that will allow characterization of the system's hydrogeology. This should include driller's logs for wells and test borings, any information on heads from piezometers and wells, geologic and soils maps and sections, and, especially, measures of hydraulic conductivity (piezometer test, aquifer tests, even specific capacity tests). Develop as thorough a conceptual model for the groundwater system as the data allow. The higher the conductivity of units between the stress and the water body of interest, the broader the monitoring array will need to be spread.

The following recommendations were developed for monitoring the effects of groundwater stresses on lakes.

1. Install numerous seepage meters across the bed of the surface water body. These should extend across the entire bed of a small lake. On large lakes, they should extend 4 to 5 km beyond the stress.
2. Read them as close to time synchronously as possible. If not possible, establish control sites which are monitored continuously throughout the study period and correct non-synchronous readings to a consistent time.
3. Install two to four piezometers nests at the shoreline. The nests must fully penetrate the geologic materials between the lake and stressed level within the aquifer system. They should extend along the shore at least over the length of the stress.
4. Monitor seepage meters and piezometers during a period when surface water level fluctuations and groundwater recharge are minimal.

The following recommendations were developed for monitoring the effects of groundwater stresses on rivers.

1. Install fully penetrating nests of piezometers along the length of channel underlain by the stress. Ideally they should occur on both banks and each nest should be adjacent to a seepage meter site.
2. Install one or two shallow piezometer nests along a control length of the channel (outside influence of stress, but with similar hydrogeology).
3. Select at least 12 stations for seepage meter installation along the length of the channel over the stress in the aquifer and at least 1 to 2 km beyond the stress.
4. Select another six to 12 stations along the control reach of the channel.
5. At each meter station install two to six meters simultaneously on a transect across the channel.
6. Monitor the seepage meters and piezometers during dry periods and when there are no significant changes in river level. This will require determining if there are any water control structures near the reach of interest.
7. Ideally, monitor all seepage and piezometer sites simultaneously, before the stress is activated and again after it has been activated. If simultaneous readings are impossible, establish and continuously monitor control seepage sites to allow for subsequent time correction. Correct

so that before and after control readings are the same. The difference between the before and after readings in the stressed reach is then the impact of the stress. If before and after monitoring is not feasible, denser arrays of meters combined with piezometer readings and the calculation methods shown in the text will produce a viable result.

REFERENCES

- Belanger, T. V., and M. T. Montgomery. 1992. Seepage meter errors, *Limnol. Oceanogr.* 37:1787-1795.
- Camber, S. L. 1994. The effects of the dewatering of Milwaukee's deep tunnel on the Milwaukee River, Milwaukee, Wisconsin. M.S. Thesis. Department of Geosciences, University of Wisconsin-Milwaukee. 238 pp.
- Cherkauer, D. S., and V. W. Bacon. 1978. Is there a ground water shortage in southeastern Wisconsin? Technical Report. Southeastern Wisconsin Regional Planning Commission,
- Cherkauer, D. S., and J. M. McBride. 1988. A remotely-operated seepage meter for use in large lakes and rivers. *Ground Water.* 26:165-177.
- Cherkauer, D. S. and B. Zvibleman. 1981. Hydraulic connection between Lake Michigan and ground-water aquifers in southeastern WI. *Ground Water.* 19:376-381.
- Hvorslev, M. J. 1951. Time lag and soil permeability in groundwater observations. U.S. Army Corps of Engineers, Waterways Experiment Station Bulletin No. 36. U.S. Army Corps of Engineers. 51 pp.
- Linnemanstons, L. 1996. Three-dimensional simulation of the hydrogeologic effects of the deep tunnel in northeastern Milwaukee Co., WI. M.S. Thesis. Department of Geosciences, University of Wisconsin-Milwaukee.
- McBride, J. M. 1987. Measurement of ground-water flow to the Detroit River, Michigan and Ontario. M.S. Thesis. Department of Geosciences, University of Wisconsin-Milwaukee. 107 pp.
- McDonald, M. G., and A. W. Harbaugh. 1984. A three-dimensional finite-difference ground-water flow model. Scientific Publications, Washington, D.C.. 528 pp.
- Mikulic, D. G. 1977. A preliminary revision of the Silurian stratigraphy of southeastern Wisconsin. In: K. G. Nelson (ed.). *Geology of Southeastern Wisconsin, Guidebook.* 41st Tri-State Field Conference. pp. A-6 to A-39.
- Milwaukee Metropolitan Sewerage District. 1981. Inline storage facilities plan. Volume 4. Borehole logs. Milwaukee Metropolitan Sewerage District, Milwaukee, Wisconsin.
- Milwaukee Metropolitan Sewerage District. 1984a. Northshore interceptor geotechnical report. Volume 3. Contract documents. Milwaukee Metropolitan Sewerage District, Milwaukee, Wisconsin.

- Milwaukee Metropolitan Sewerage District. 1984b. Cross Town interceptor geotechnical report. Volume 3. Contract Documents. Milwaukee Metropolitan Sewerage District, Milwaukee, Wisconsin.
- Ostrom, M. E. 1967. Paleozoic stratigraphic nomenclature for Wisconsin. Information Circular No. 8. Wisconsin Natural History and Geological Survey, Madison, Wisconsin.
- Rodenbeck, S. . 1988. Merging Pleistocene lithostratigraphy with geotechnical and hydrogeologic data - Examples from southeastern WI. M.S. Thesis. Department of Geology and Geophysics, University of Wisconsin-Madison.
- Rovey, C. W., II. 1990. Stratigraphy and sedimentology of Silurian and Devonian carbonates, eastern Wisconsin, with implications for ground-water discharge into Lake Michigan. Ph.D. dissertation. University of Wisconsin-Milwaukee. 427 pp.
- Rovey, C. W., II, and D. S. Cherkauer. 1994a. Relation between hydraulic conductivity and texture in a carbonate aquifer: Observations. *Ground Water*. 32(1):53-62.
- Rovey, C. W., II, and D. S. Cherkauer. 1994b. Relation between hydraulic conductivity and texture in a carbonate aquifer: Regional continuity. *Ground Water*. 32(2):227-238.
- Rovey, C. W., II, and D. S. Cherkauer. 1995. Scale dependency of hydraulic conductivity measurements. *Ground Water* 33(4):769-790
- Schulz-Makuch, D. 1996. Effects of heterogeneities and scale of measurement on dispersivity and hydraulic conductivity variations in the dolomite aquifer of the Milwaukee area, WI. Ph.D. Dissertation. Department of Geosciences, University of Wisconsin-Milwaukee.